Talbot-Lau X-ray Deflectometry:
A refraction-based imaging diagnostic for HED experiments at the LLE

M. P. Valdivia
Center for Energy Research, University of California San Diego
Department of Physics and Astronomy, The Johns Hopkins University

NNSA HEDLP Grants: DE-NA0001835, DE-NA0002955, DE-NA0003882, DE-NA0004028
NNSA NLUF Grants: DE-NA0003526, DE-NA0003941, and shot time for FY22-23
DoE Office of Science FES: DE-SC0020005 LaserNetUS (Omega Laser Facility)

Collaborators

D. Stutman*
Department of Physics and Astronomy, The Johns Hopkins University
**Now at Extreme Light Infrastructure - Nuclear Physics Center (ELI-NP)*

C. Stoeckl, C. Mileham, W. Theobald, D. Haberberger, A. Shvydky, I. A. Begishev, S. Fess, T. Filkins, M. Romanofsky, S. P. Regan
Laboratory for Laser Energetics, University of Rochester

A. Casner[1], V. Bouffetier[1*], G. Perez-Callejo [2**], G. Rigon[2], B. Albertazzi[2], P. Mabey[2], T. Michel[2], M. Koenig[2]
[1]CEA, DAM, DIF, F-91297, Arpajon / CELIA, University of Bordeaux, France,
[2]LULI, École Polytechnique, CNRS, CEA, UPMC, route de Saclay, F-91128 Palaiseau, France
**Now at European XFEL GmbH ; **Now at Universidad de Valladolid, Valladolid, Spain*

S. R. Klein, P. A. Keiter*, J. R. Fein**, R. Melean, C. Kuranz, M. Trantham, R. P. Drake
Department of Climate and Space Sciences and Engineering, University of Michigan, Ann Arbor
**Now at LANL ; **Now at SNL*

S. Sander, T. Ebert, G. Schaumann
Laser- und Plasmaphysik, Institut für Kernphysik, Technische Universität Darmstadt

G. Collins IV*, F. Conti, M. Bailly-Grandvaux, F. N. Beg
Center for Energy Research, University of California San Diego
**Now at General Atomics*

M. Vescovi*, F. Veloso, M. Favre, E. S. Wyndham
Instituto de Física, Pontificia Universidad Católica de Chile, Chile
**Now at Helmholtz Zentrum Dresden Rossendorf*

Big thanks to LLE staff too!

Omega EP (Dave, Mingsheng), MTW (Bob, Jake), Target Fab. (Julie, Mark), XOPS (Mike, Mason, Jeff, et al.), EP diagnostics (Danielle, Mike, Corey, Jim, Steve, Chad), Engineering (Chuck, Jun), Safety (Walter, Doug), Admin. (Jean, Kim, Lori), +many more…

X-ray Imaging diagnostics

Center for Energy Research
Johns Hopkins University

Electron density diagnostics for HED/ICF

For low-Z matter probed at 1-100 keV: ***Refraction* signatures >> *Attenuation***

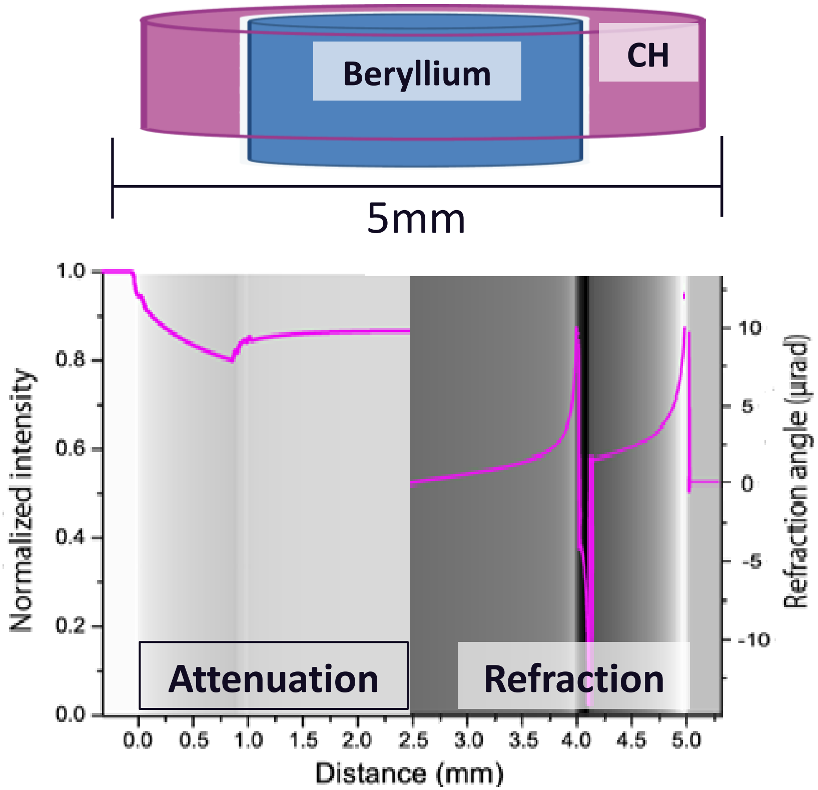

Complex Optical Index:

$$N = 1 - \delta + i\beta$$

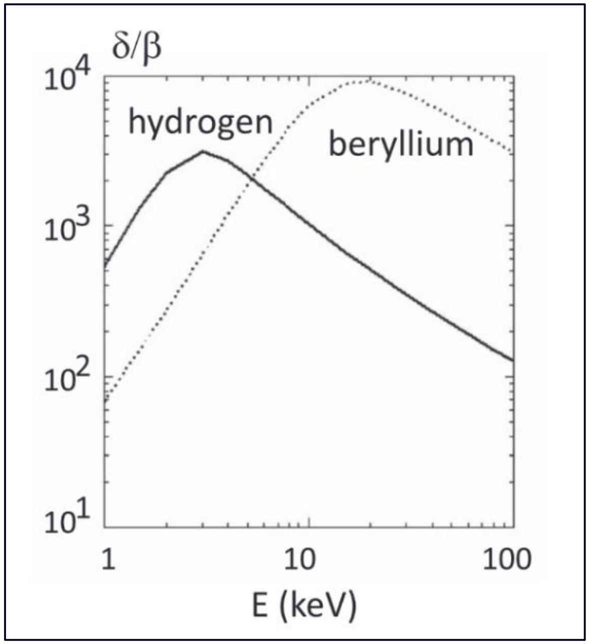

XWFP simulation: T. Weitkamp, *Advances in Computational Methods for X-Ray and Neutron Optics* (2004)

TL for HEDP: Stutman et al, *Rev. Sci. Instrum*. **82**, 113508 (2011)

Refraction-based diagnostics

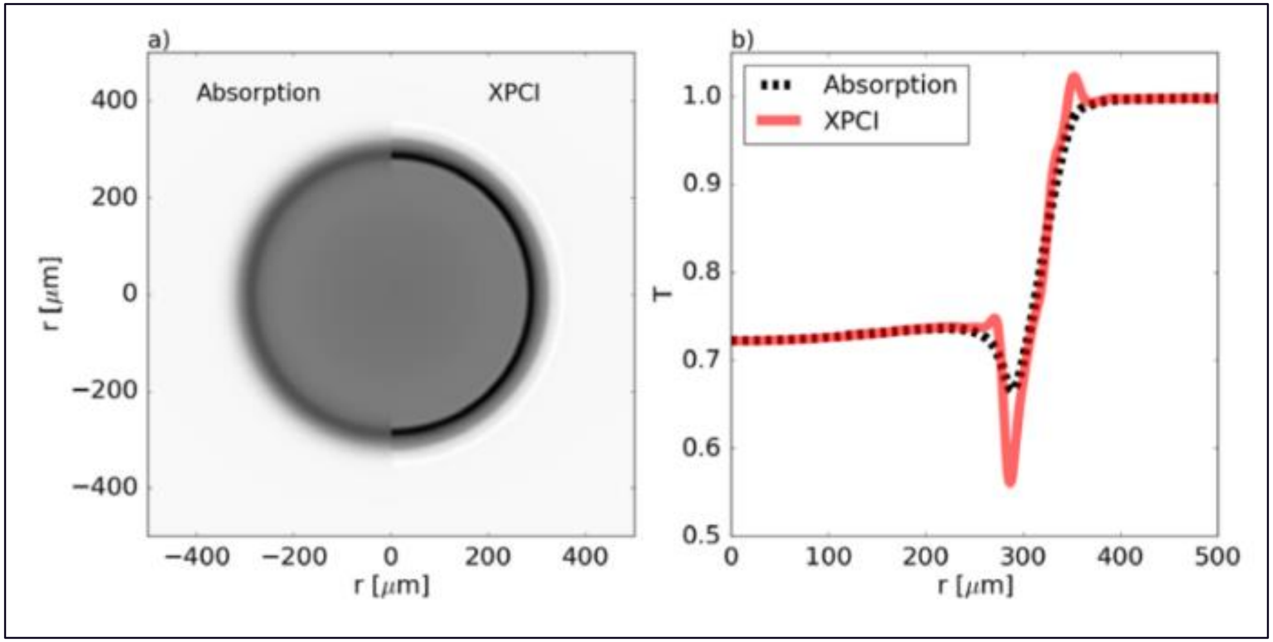

Simulation: D. Cao (LLE). Post-processing L. Antonelli (York Plasma Physics Institute) and F. Barbato (CELIA)

LILAC simulation of a CH shell post-processed to compare Phase-Contrast imaging using long length propagation (XPCI) vs absorption radiographs with 15 µm source

Information extracted from x-ray refraction angle:

$$\alpha(x, y) = \lambda/2\pi\Delta\Phi(x, y)$$

Phase change

$$\phi = -\frac{1}{2N_c}\int_0^L \nabla N_e \, dl$$

Electron density

Talbot-Lau interferometry

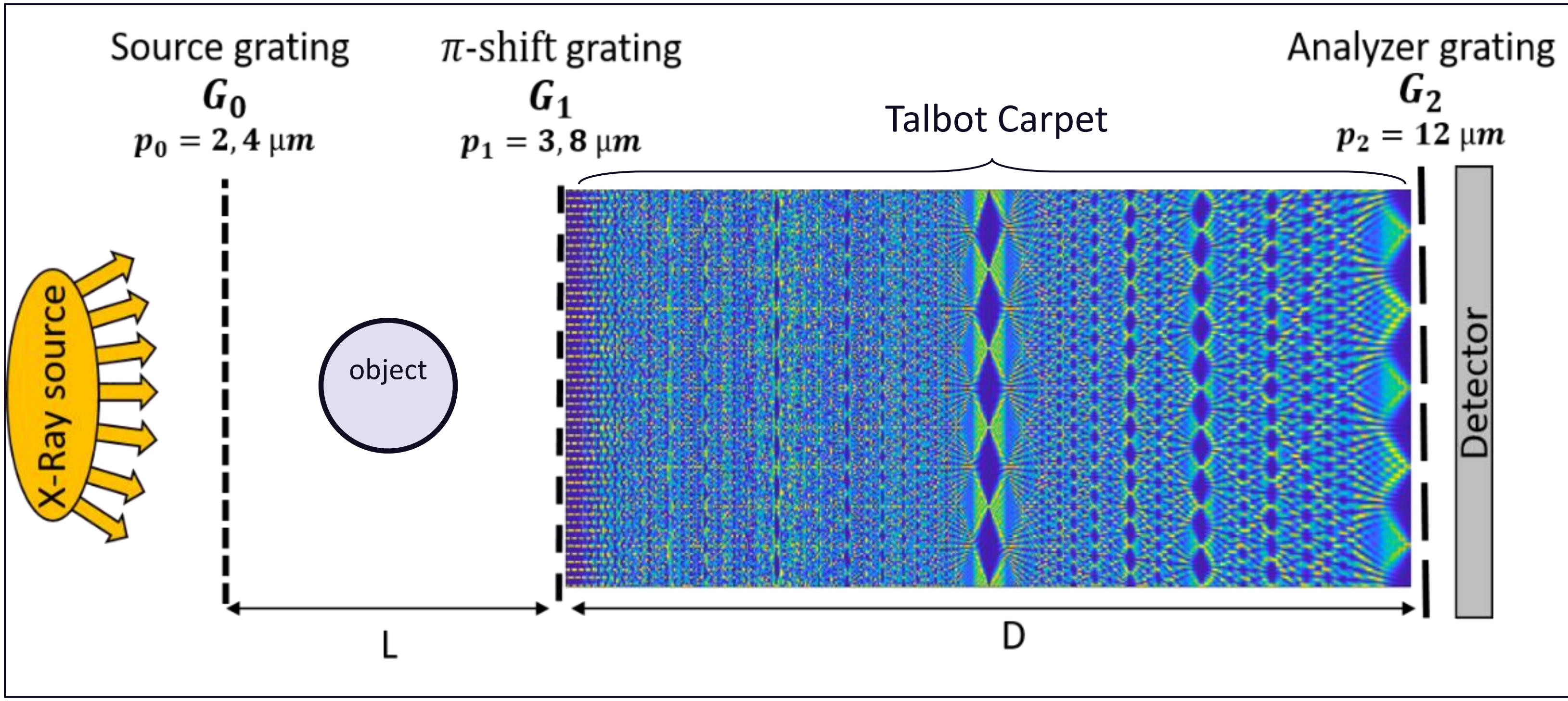

Talbot-Lau unperturbed and perturbed pattern by a PMMA rod performed with a 8keV X-ray tube

Talbot length:

$$z_T = \frac{1}{1-\sqrt{1-\frac{\lambda}{p_1^2}}} \approx \frac{2p_1^2}{\lambda^2}$$

G_2 position: $D = M_T \frac{m z_T}{4\eta^2}$

With: $\eta = \begin{cases} 1\,,\ \pi/2\ shift\ grating \\ 2\,,\ \pi\ shift\ grating \end{cases}$

Talbot magnification:

$$M_T = \frac{L+D}{L}$$

Talbot-Lau X-ray Deflectometry

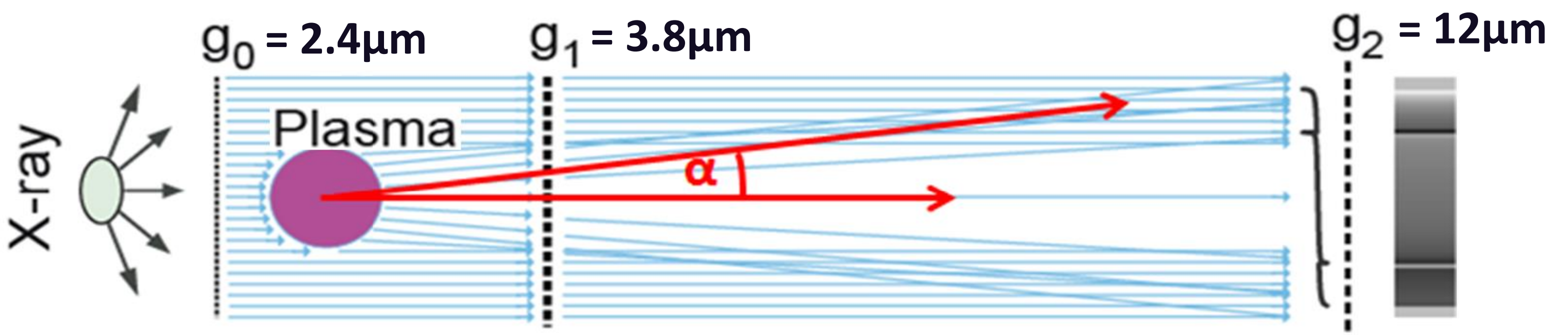

TL for HEDP: Valdivia et al., *Journal Appl. Phys.* **144** (2013); Ibid., *RSI* **85** (2014)

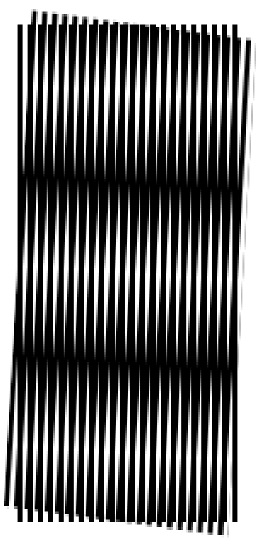

- (small) Grating rotation -> Moiré fringes:

  Period ≈ g/θ

- Fringe shift proportional to refraction angle

$$\alpha(x,y) = \frac{r_e \lambda^2}{2\pi} \frac{\partial}{\partial x} \left[\int N_e (x,y,z)\, dz\right]$$

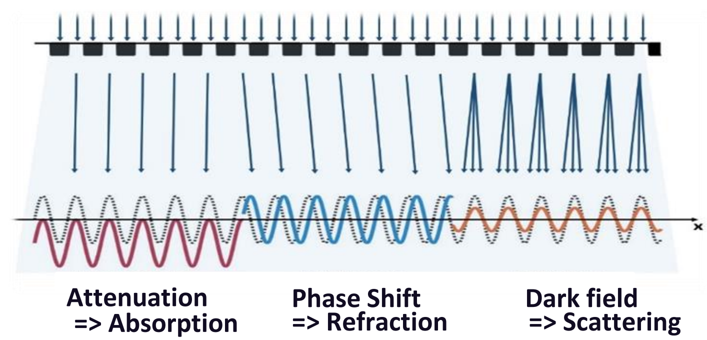

XWFP simulation: 8 keV TXD of CH shell

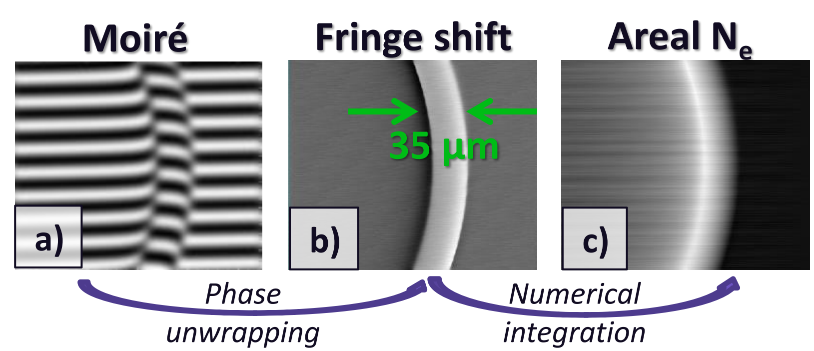

Simultaneous information

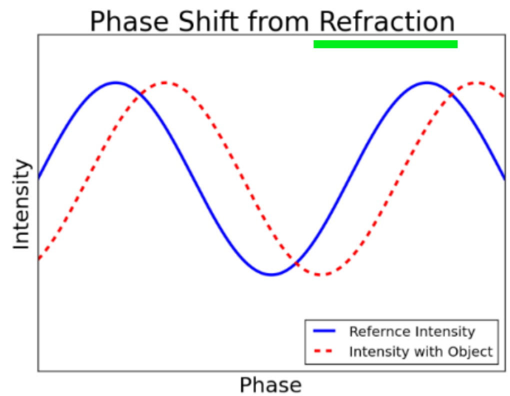

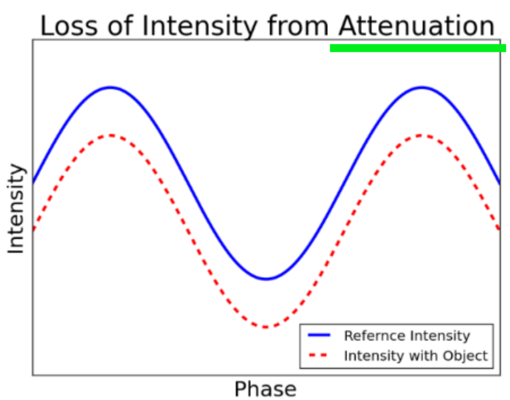

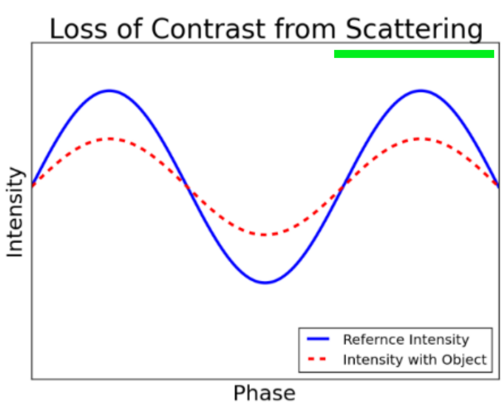

Fourier decomposition:

$$I(x,y) = a_0 + a_1 \cos(\{2\pi/ P_M\} + \psi)$$

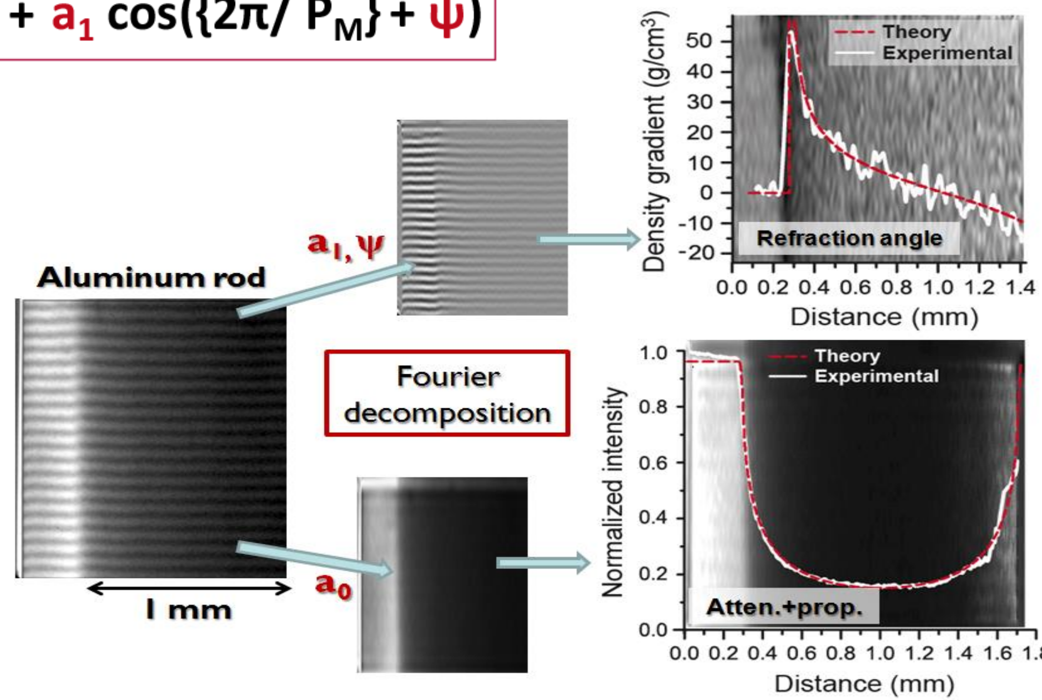

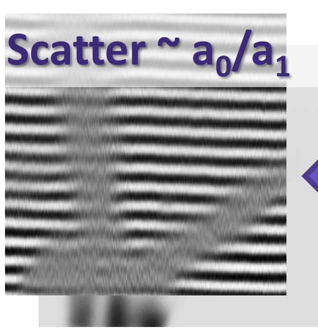

Moire

Loss of coherence

Scatter due to micro-structures ($\sim G_0$ period order)

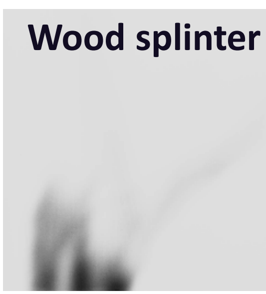

Propagation

Measurements of n_e gradient

Be rod

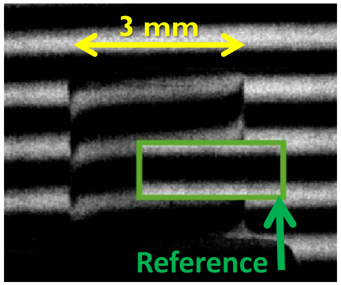

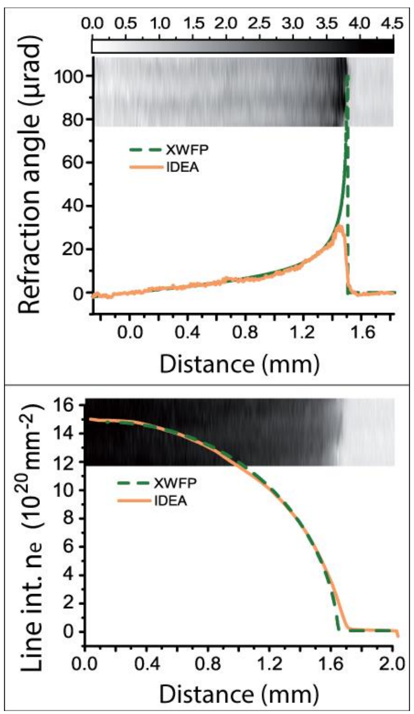

- Strong signature of n_e gradients and interfaces
- Spatial resolution
  - Horizontal: Source-size
  - Vertical: ~ Period

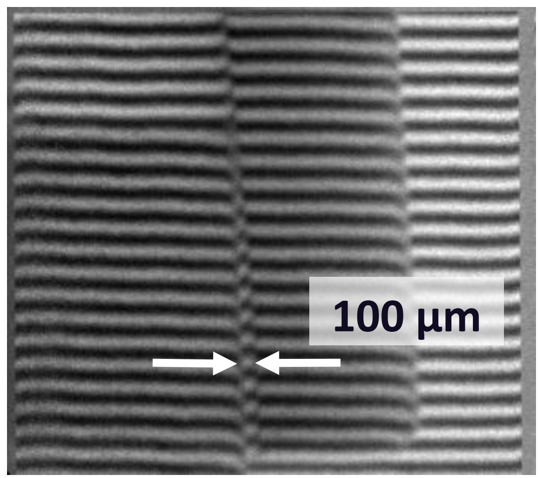

17keV x-ray medical tube

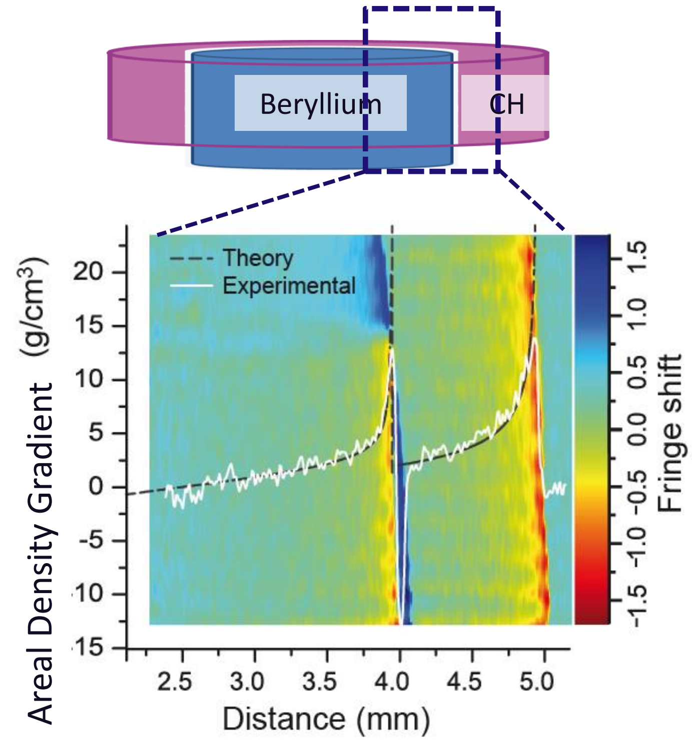

Talbot-Lau: Valdivia et al., *RSI* (2014)

Accurate detection of interfaces and (sharp and mild) n_e gradients in low-Z matter.

*n_e measurement dynamic range

$$\frac{\Delta(N_e L)}{\Delta x} \approx \frac{2.2\times10^{29}}{\lambda^2{}_{Angs}}\cdot\alpha \approx \frac{2.2\times10^{29}}{\lambda^2{}_{Angs}}\cdot\frac{g_0}{P}\cdot F$$

Fringe shifts detection: few % to several periods.

*Where refraction angle ‘α’ is equivalent to fringe shift ‘F’ scaled by the interferometer effective angular resolution ‘W_{eff}’ (g_0 period and g_0 to plasma distance ‘p’ ratio).

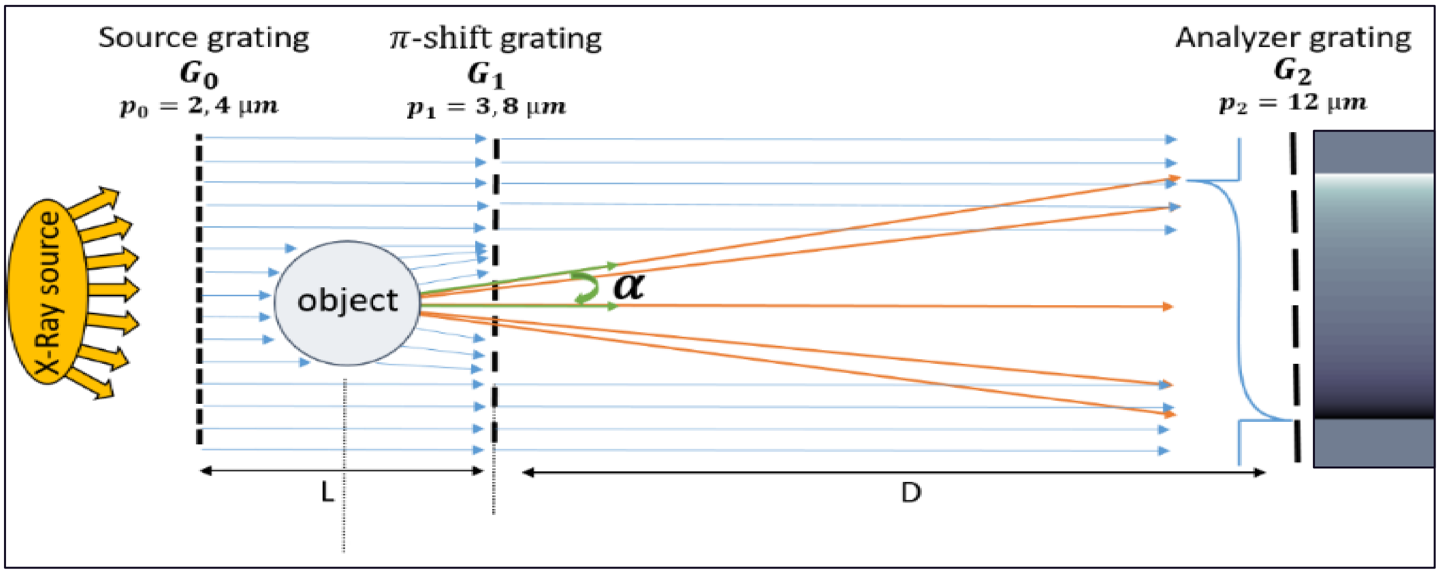

For a CH shell ~200 µm → i) 0.1x solid n_e ->(few keV)
ii) >100x solid n_e -> (~20 keV)

$Z_{average}$: composition (mixing)

Center for Energy Research

Johns Hopkins University

$$\beta(x,y,z) = r\delta(x,y,z).$$

$$\delta = (r_0/2\pi)\lambda^2 n_a (Z + f').$$

$$\beta = (r_0/2\pi)\lambda^2 n_a f'',$$

$$\mu = -\ln(I/I_0)/L,$$

$$\Delta\Phi(x,y) = 2\pi\delta L/\lambda,$$

$$\boxed{r = -\ln(I/I_0)/(2\Delta\Phi).}$$

'r' ~third degree polynomial of Z_{avg}

Fluorocarbon fiber

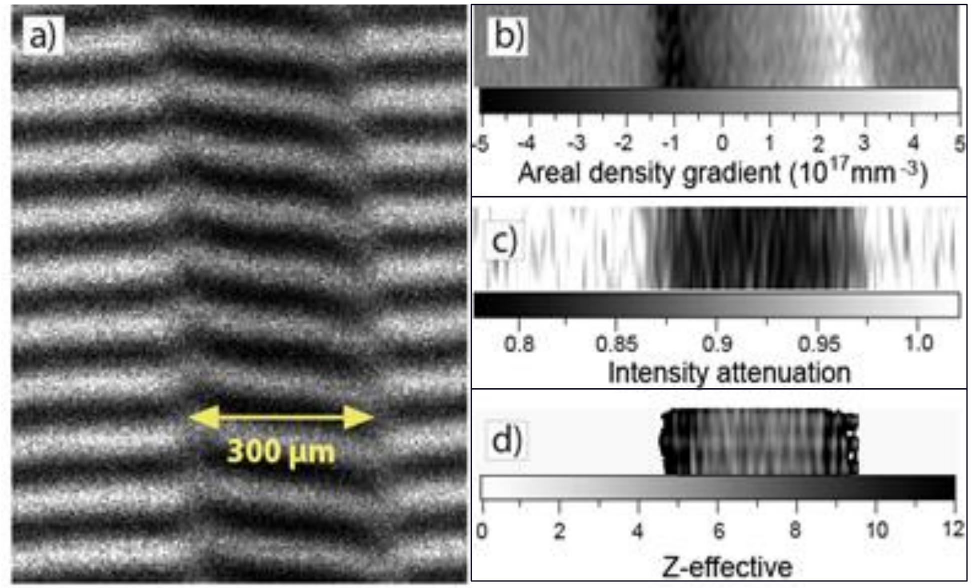

Z-average: Valdivia et al., *Applied Optics* **54** (2014)

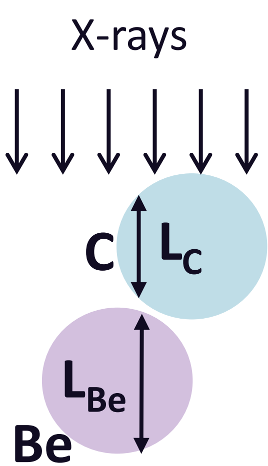

$$\langle Z_{avg}\rangle \approx (f_C Z_C^3 + f_{Be} Z_{Be}^3)^{1/3}\ ; \quad f_i \equiv L_i / \sum L_i$$

Attenuation Refraction Attn./ Refr.

Adaptation to HEDLP

Demonstrate n_e diagnostics in high-intensity laser environment:

- Grating survival
- Talbot pattern formation
- Refraction measurement
- Electron density retrieval

- **Laser:** 10-150 J, 8-30 ps
  MTW, LULI2000, ECLIPSE (200mJ, 30fs), **OMEGA-EP**

- **Targets**
  - Cu foil:
    - 500 x 500 x 20 μm^3
    - 200 x 200 x 12.5 μm^3
  - Cu wire: 20 μm diameter
    (backed by 500 x 500 x 12.5 μm^3 Polymide)
  - Cu grain: ~14-40 μm diameter
    (backed by 500 x 500 x 12.5 μm^3 Polymide)
  - Bookend targets (Cu wire and CH foils)

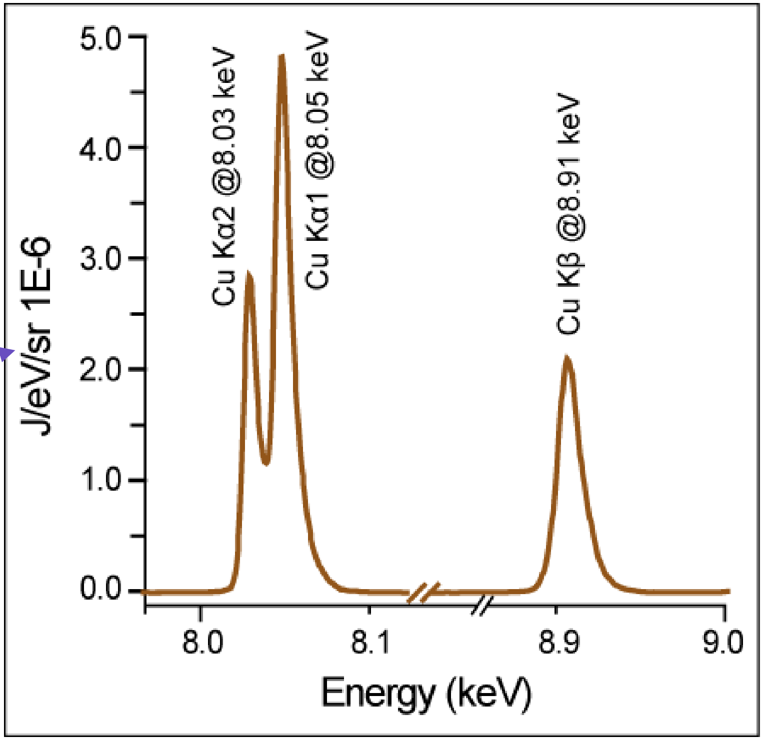

TXD backlighters (MTW): Valdivia et al., *RSI* **87** 023505 (2016)

MTW: laser-driven backlighter

Center for Energy Research

Johns Hopkins University

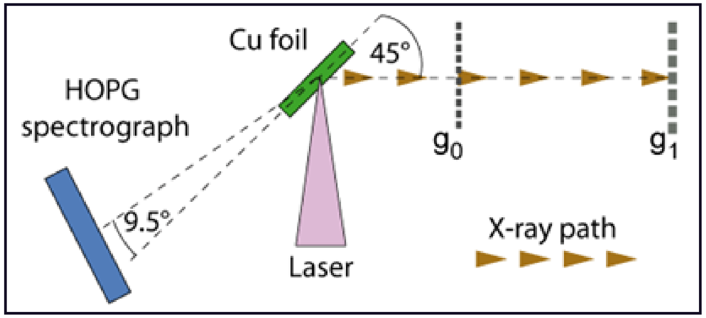

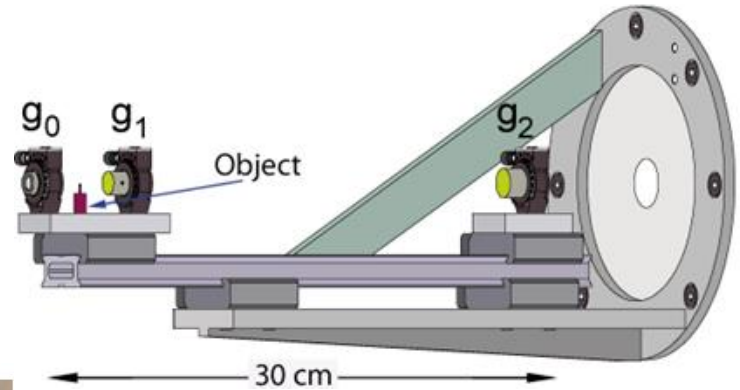

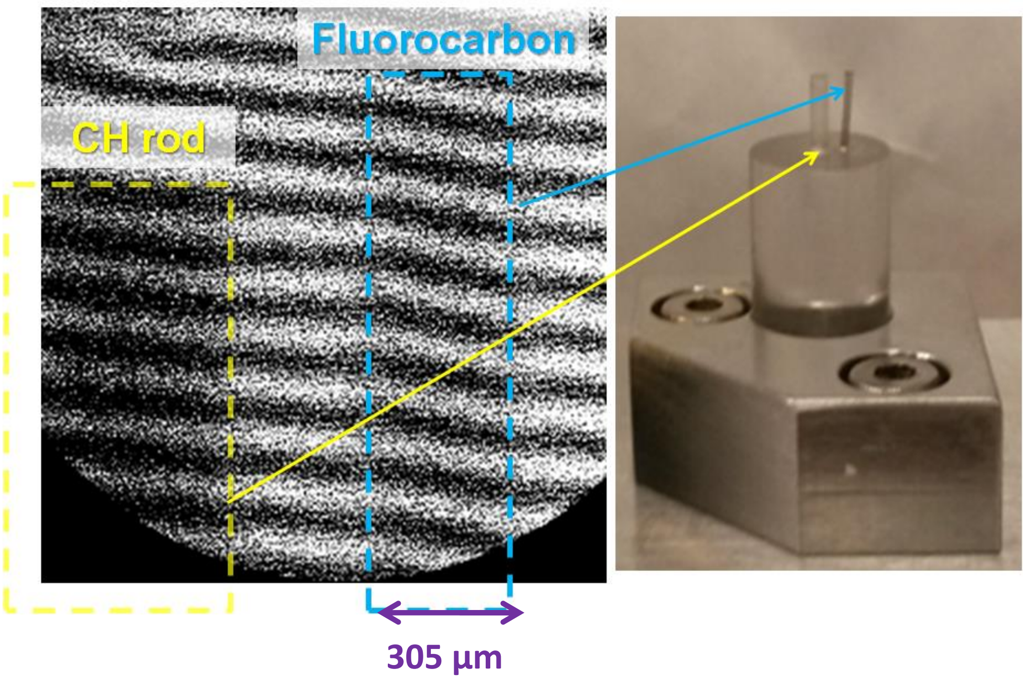

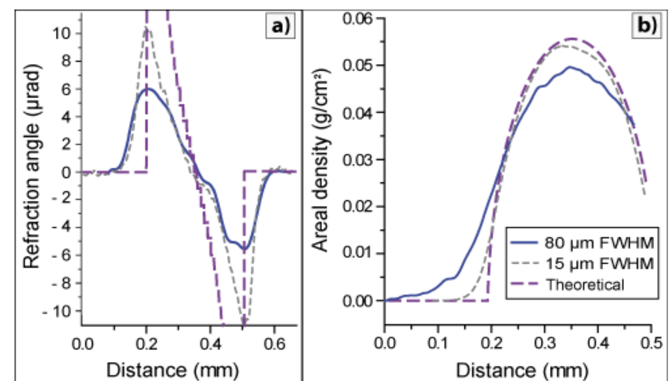

TL (laser backlighter): Valdivia et al., *IEEE TPS* **44** (2016)

Areal density: **0.050 g/cm²**

Density: **1.66 g/cm³** (~10% error)

MTW: X-ray backlighter studies

Center for Energy Research

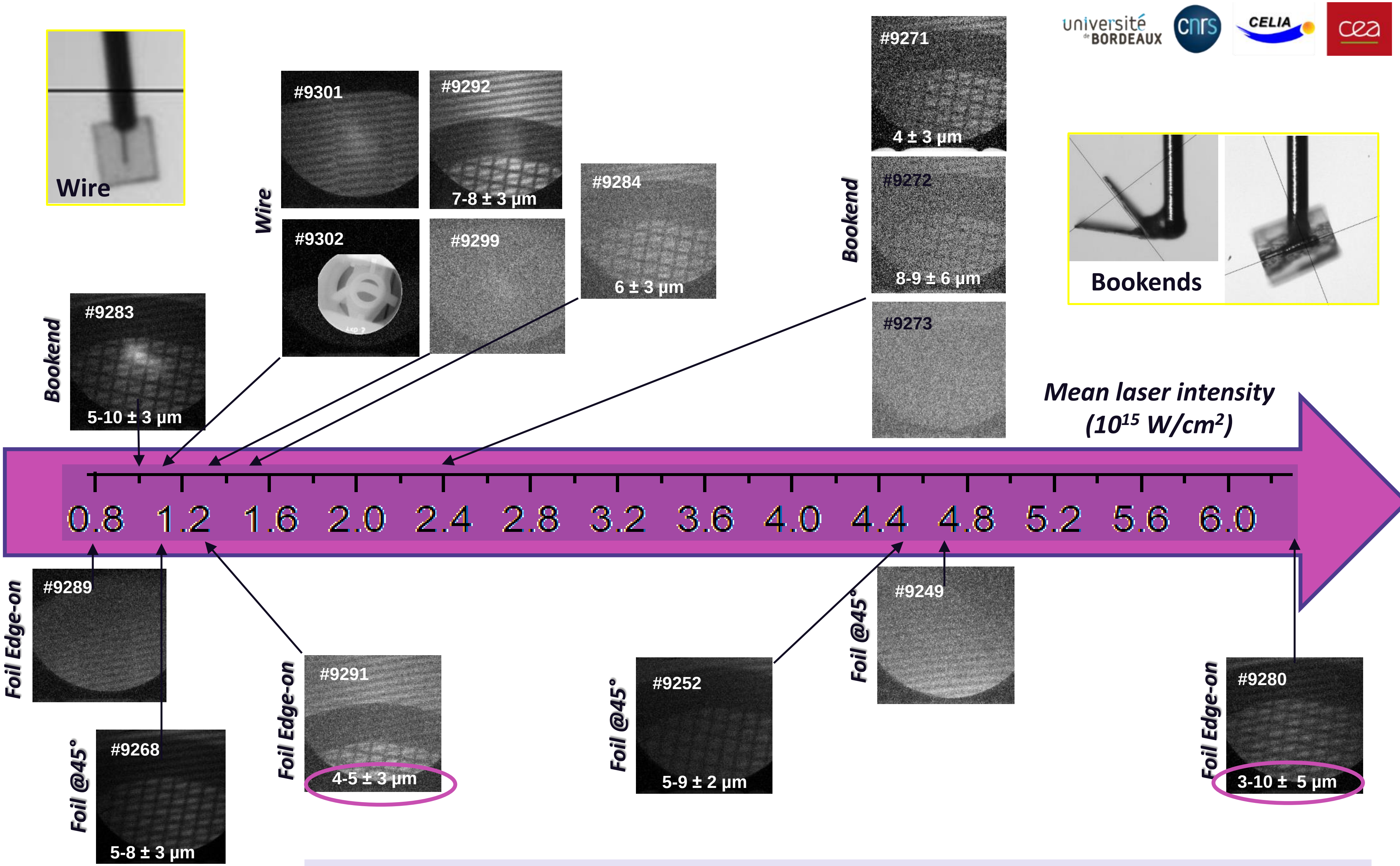

Lower contrast (32% vs. 22%). High energy emission from "micro-backlighters" (*hot electrons*)

*Conversion efficiency: Cu BL

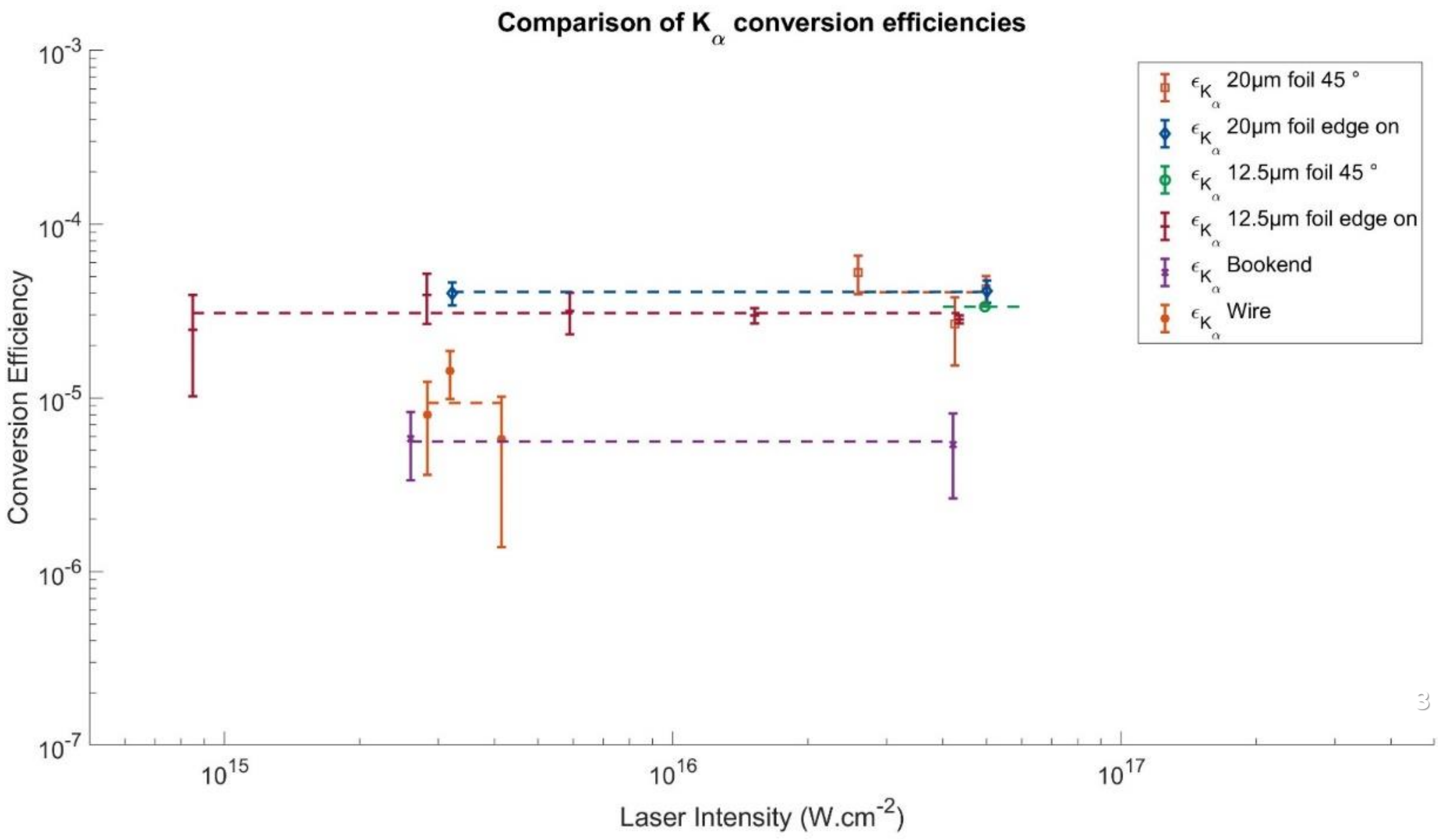

Ablation studies on Omega EP

- <u>Motivation</u>: Investigate dependence of LPIs, such as two-plasmon decay, on plasma conditions
- TXD: image the <u>plasma corona</u> near critical density for long-pulse laser-plasma experiments (from $n_c/10$ to n_c)

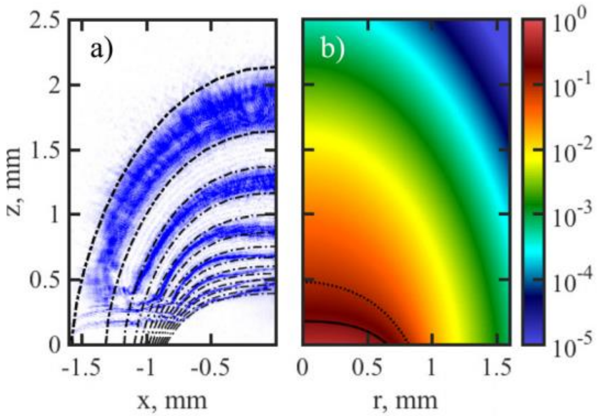

Hot electron mitigation: J. Fein, *PoP* **24** (2017)
(a) AFR data. (b) Electron density profile.

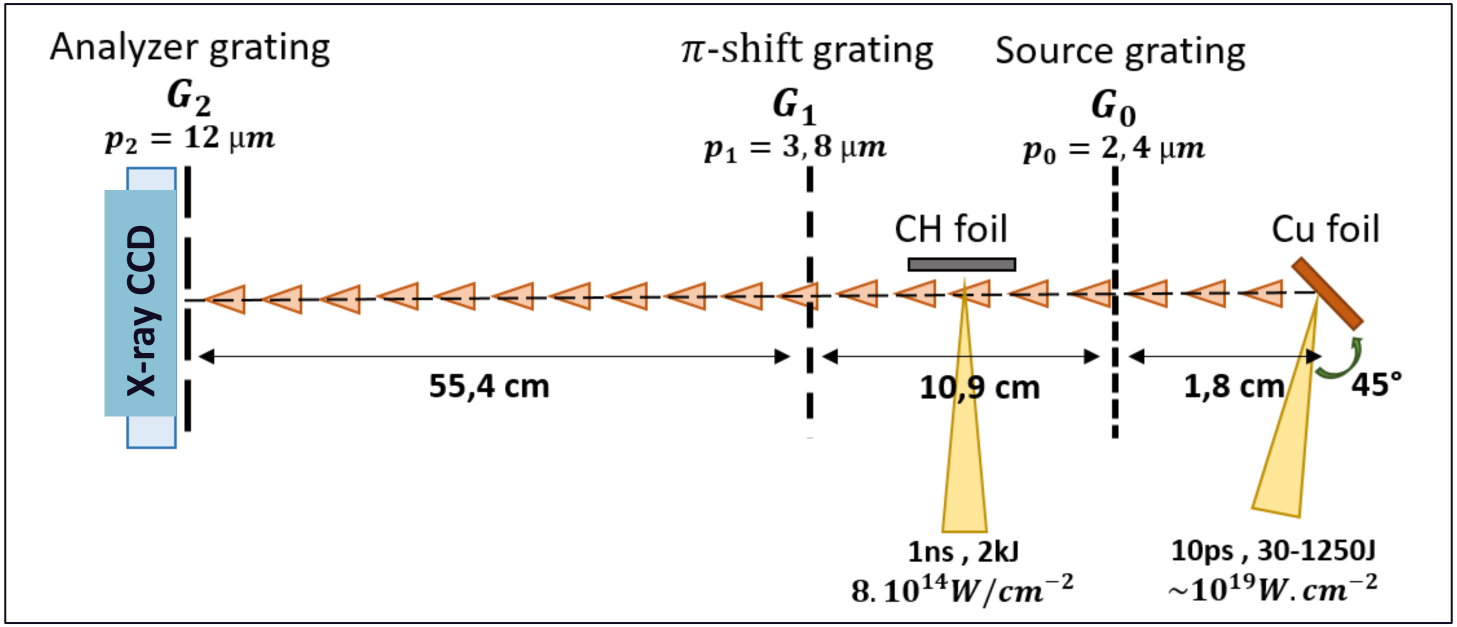

*Preliminary exps: LULI2000

First shots with plasma target:

- Test grating survival
- Demonstrate Moiré fringe formation

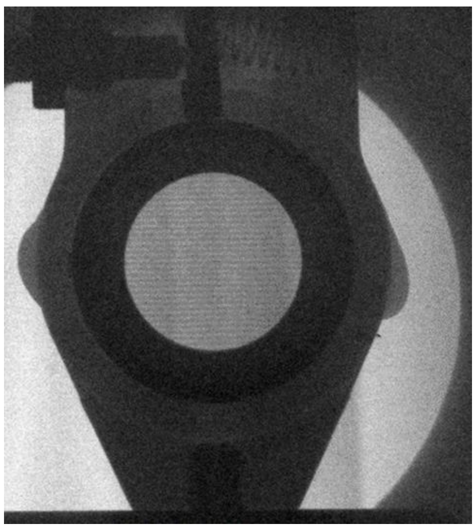

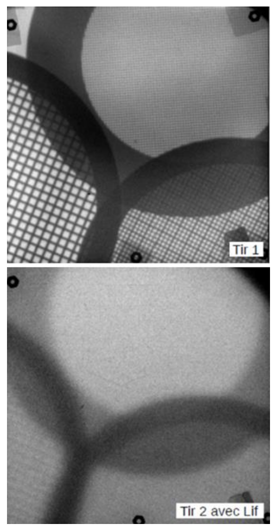

7% contrast with imaging plates

(>27% with XR tube)

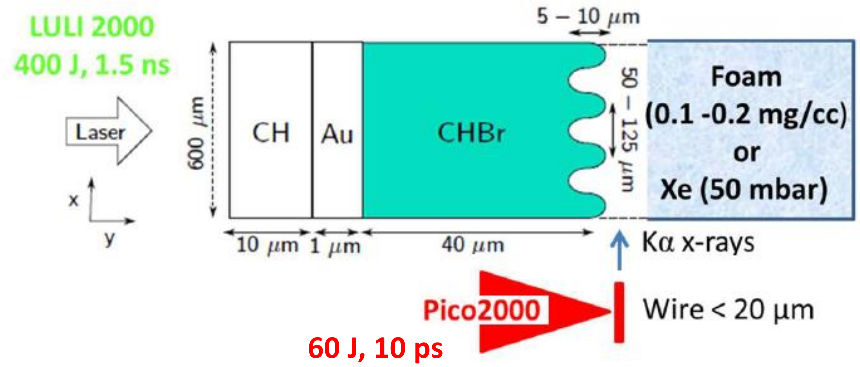

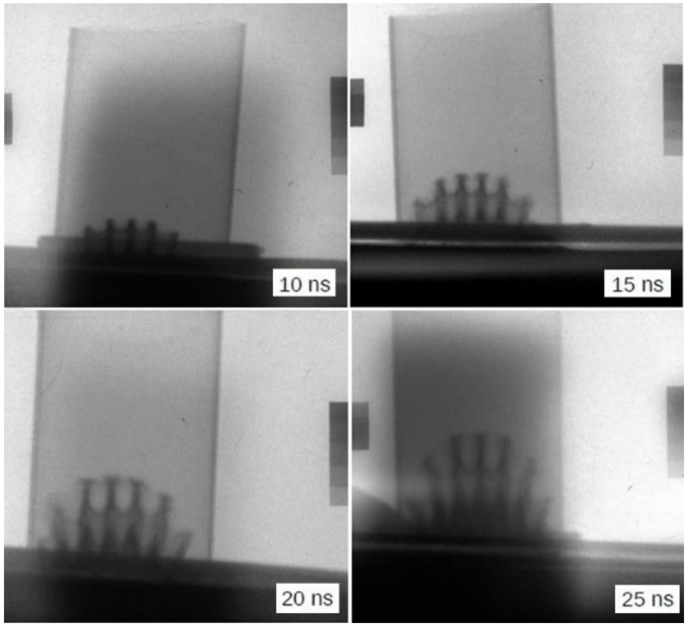

Experimental platform

CER Center for Energy Research

Johns Hopkins University

- Talbot order m=7 (~70 cm long)
- Rails pre-aligned at JHU (XR tube)
- Source grating g_0: ~1x1 mm² effective area

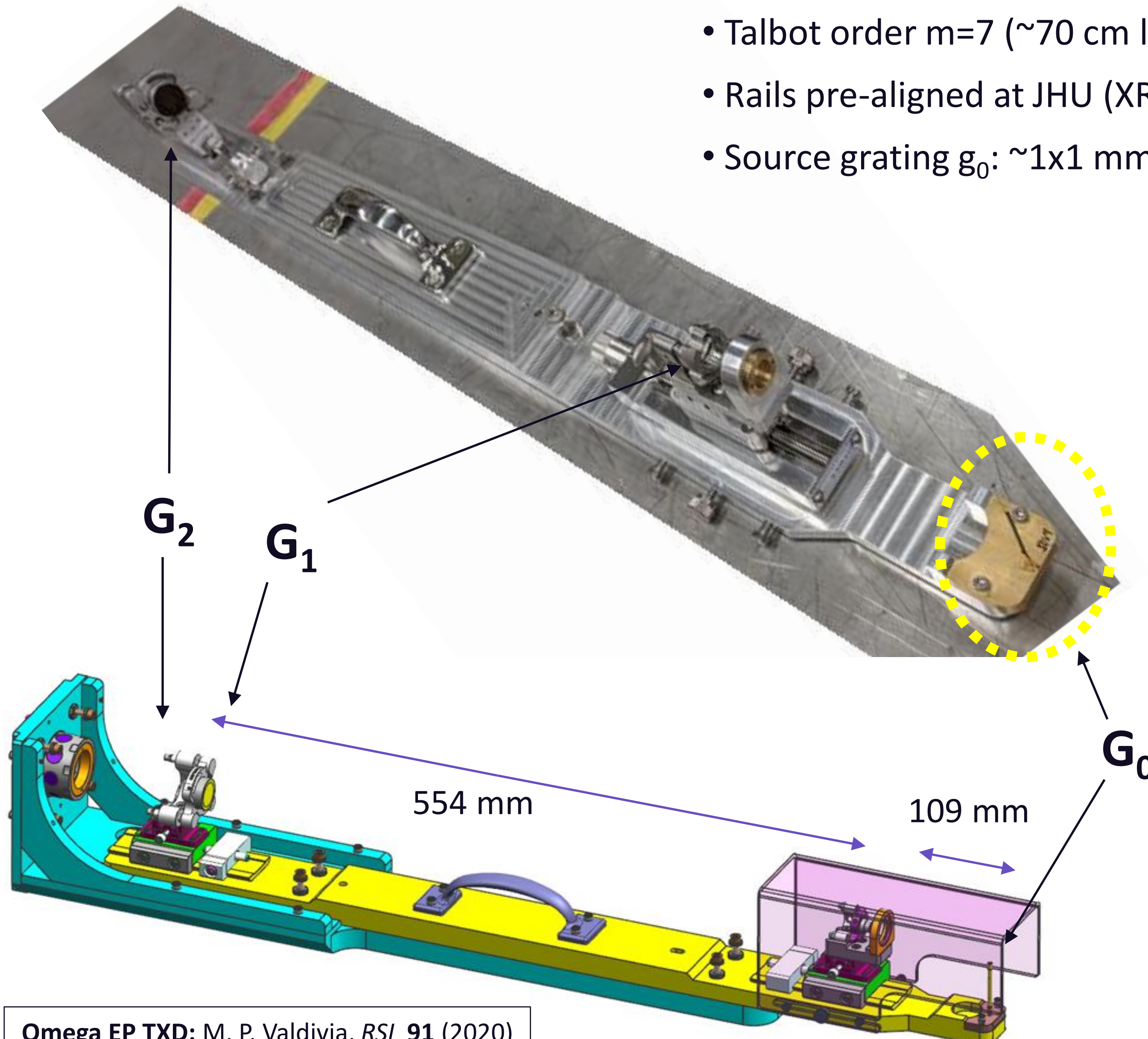

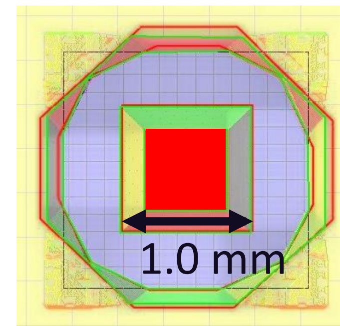

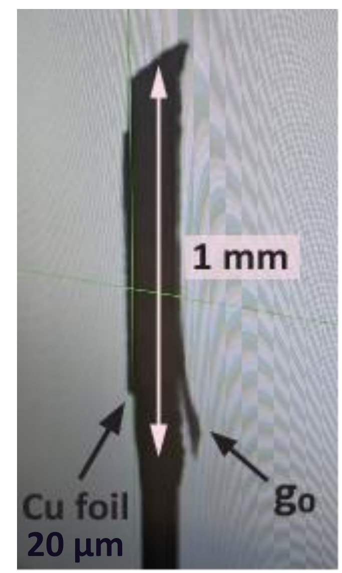

Omega EP TXD: M. P. Valdivia, *RSI* **91** (2020)

X-ray backlighter analysis: EP

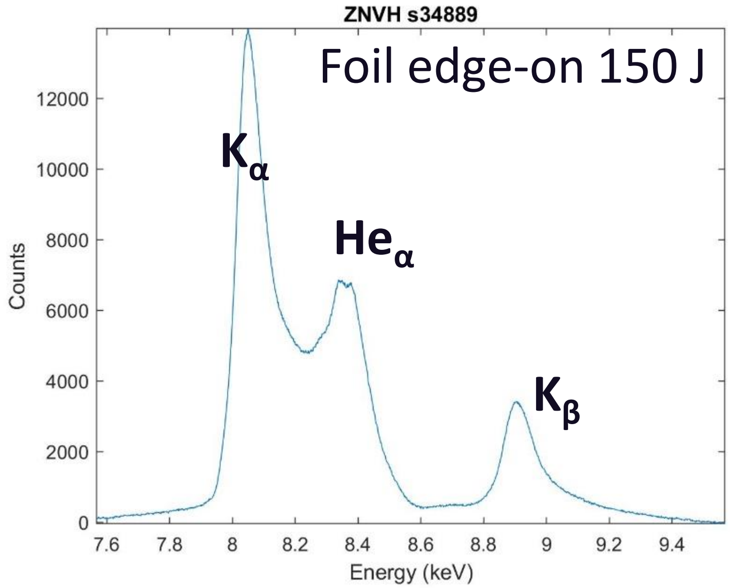

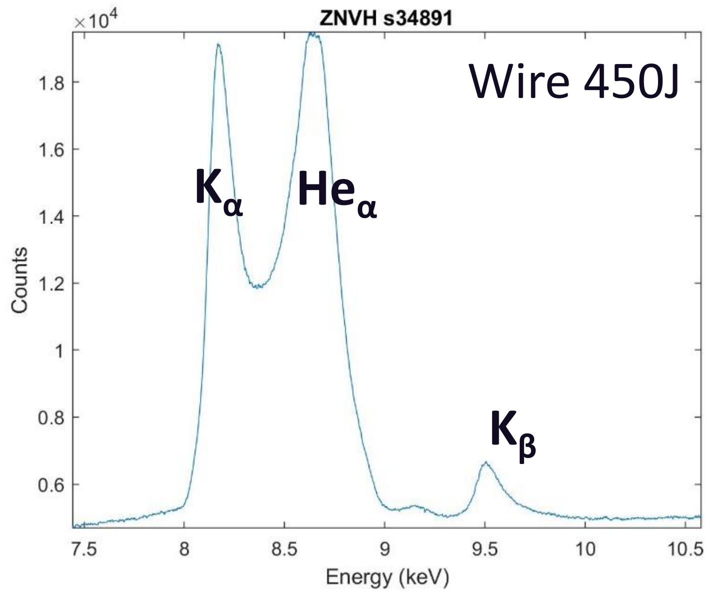

- **Laser parameters:** 50 - 450 J, 10 ps
  I ~ 10^{16-18} W/cm^2
- **Targets:**
  - 1.15 x 0.8 mm^2 x 20 µm Cu foil
    - Irradiated at 45° and normal (Edge-on)
  - 20 µm diameter Cu wire
    (backed by 1.15 x 0.8 mm^2 x 20 µm polyamide)
  - Bookend targets: Cu wire + CH foils

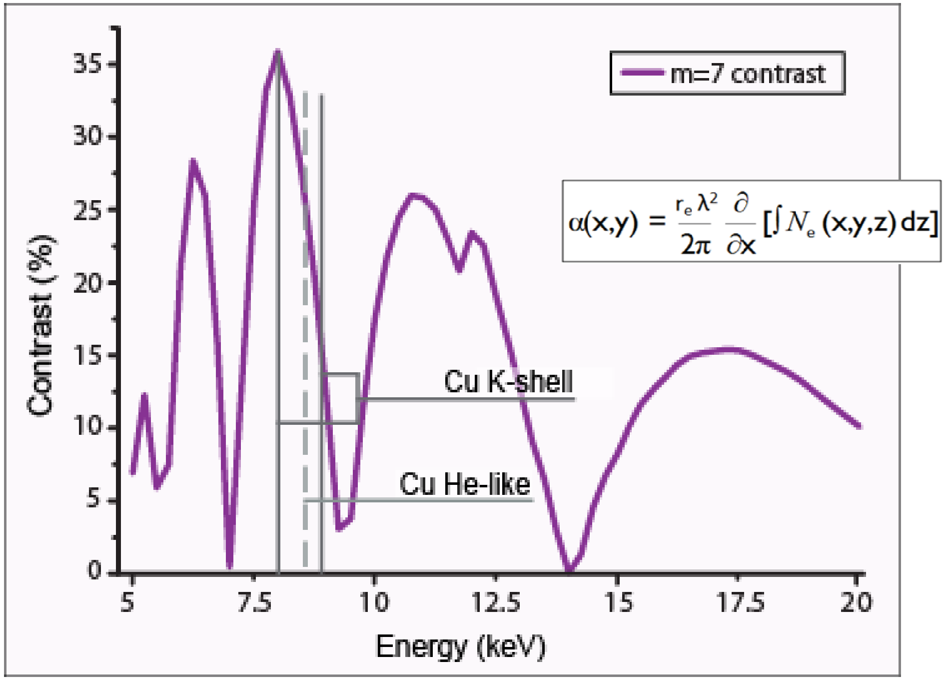

Omega EP TXD: FY18 & FY19

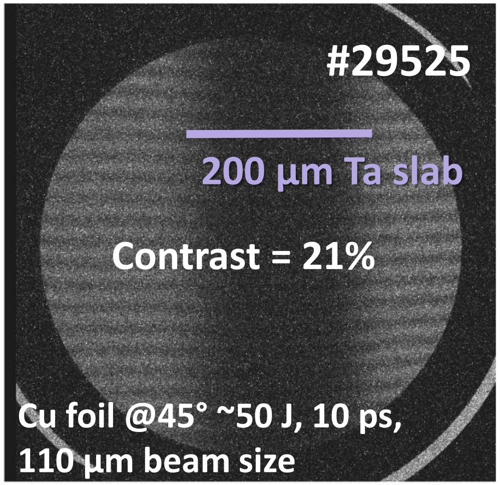

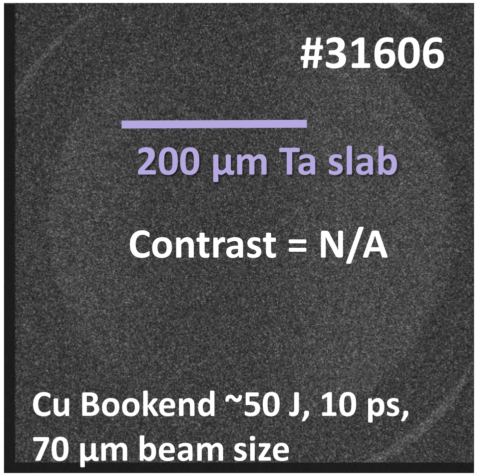

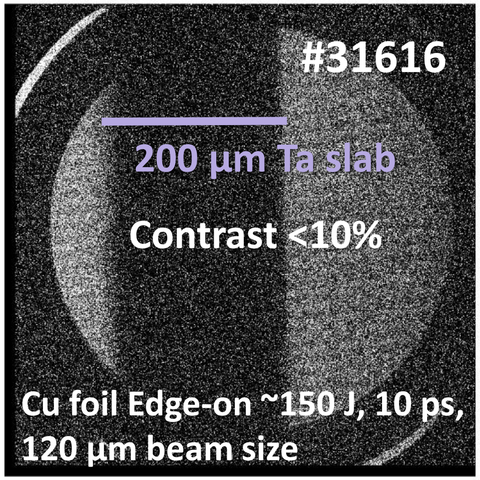

TXD for Omega EP: M. P. Valdivia, *RSI* **91** (2020)

<u>Moire fringe Contrast</u>:
Decreases with energy and "best-resolution" targets:
emission outside curve (hot electrons)

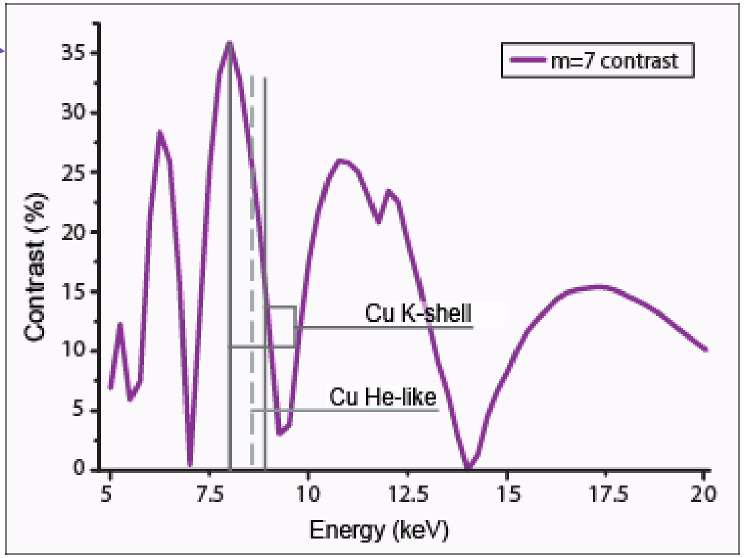

Target	I (W/cm2)	N Ka (phot)	E_Ka (J)	Conv Eff Ka	Err Conv eff
45° foil	2,36E+17	2,36E+17	1,47E-02	2,98E-04	0,60E-04
Edge on	2,79E+17	2,72E+17	3,28E-02	2,38E-04	0,48E-04

X-ray backlighter optimization:
-> Better spatial resolution: <u>maintaining contrast</u>

***Increase X-ray flux (SNR) and use monochromatic x-ray backlighting (higher energies with "best-resolution" targets)**

Nevertheless, TXD probed an expanding plasma front up to densities usually opaque to 4ω probe, for example.

Contrast: 9-14% for EP-TXD I
6-9 % for EP-TXD II
* >25% with continuous x-ray source

Resolution: 62 – 78 µm for EP-TXD I
11 – 32 µm for EP-TXD II

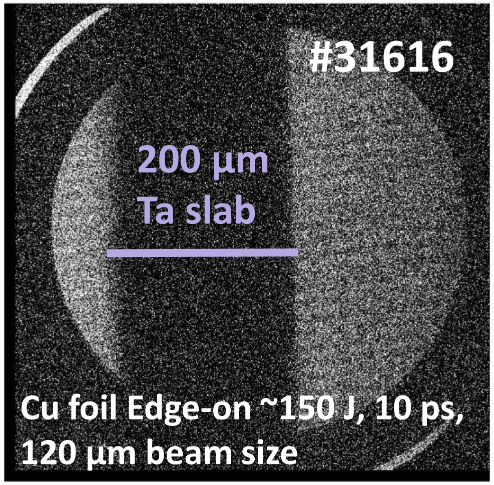

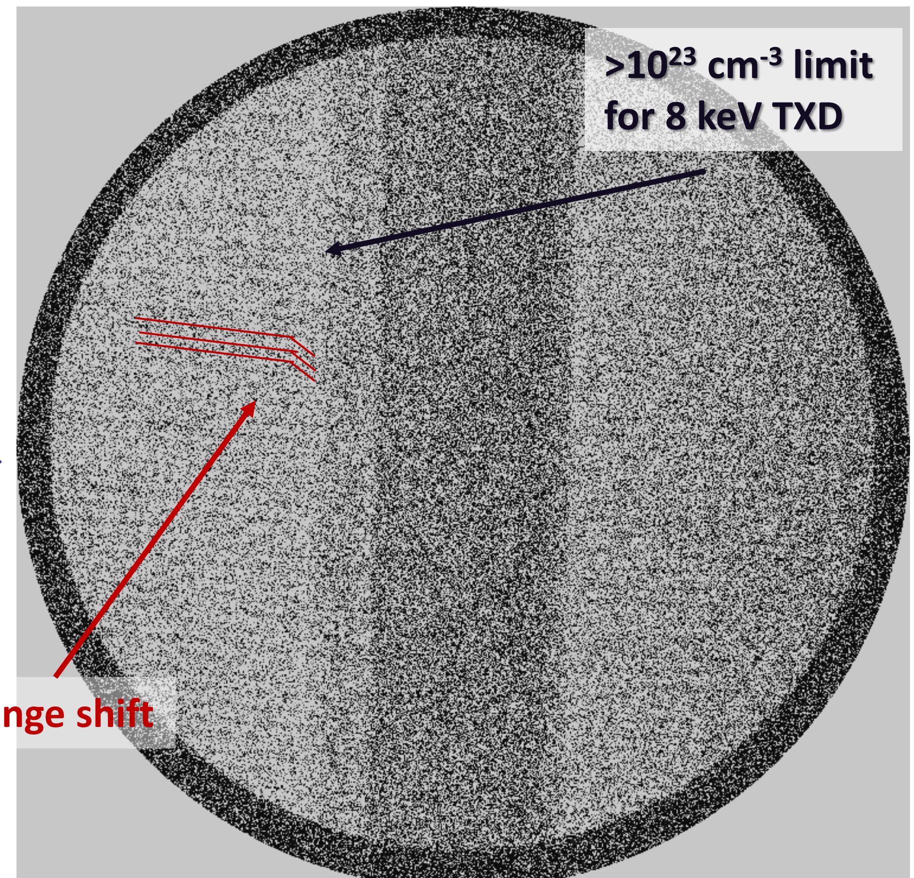

TXD for HEDP: M. P. Valdivia, *RSI* **92** (2021)

*Contrast further reduced: self-emission

X-ray refraction angle 2D map

<10% fringe contrast: Shifts tracked manually and individually.

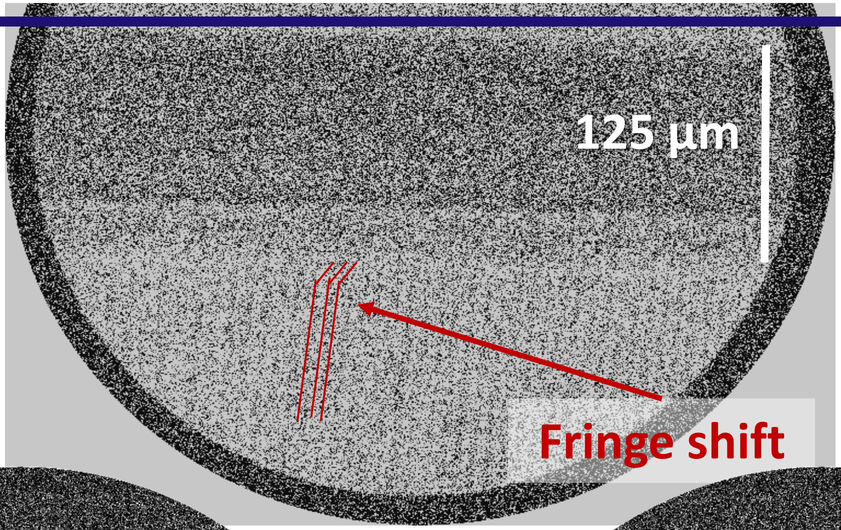

Two separate x-ray refraction angle 2D maps retrieved through TXD.

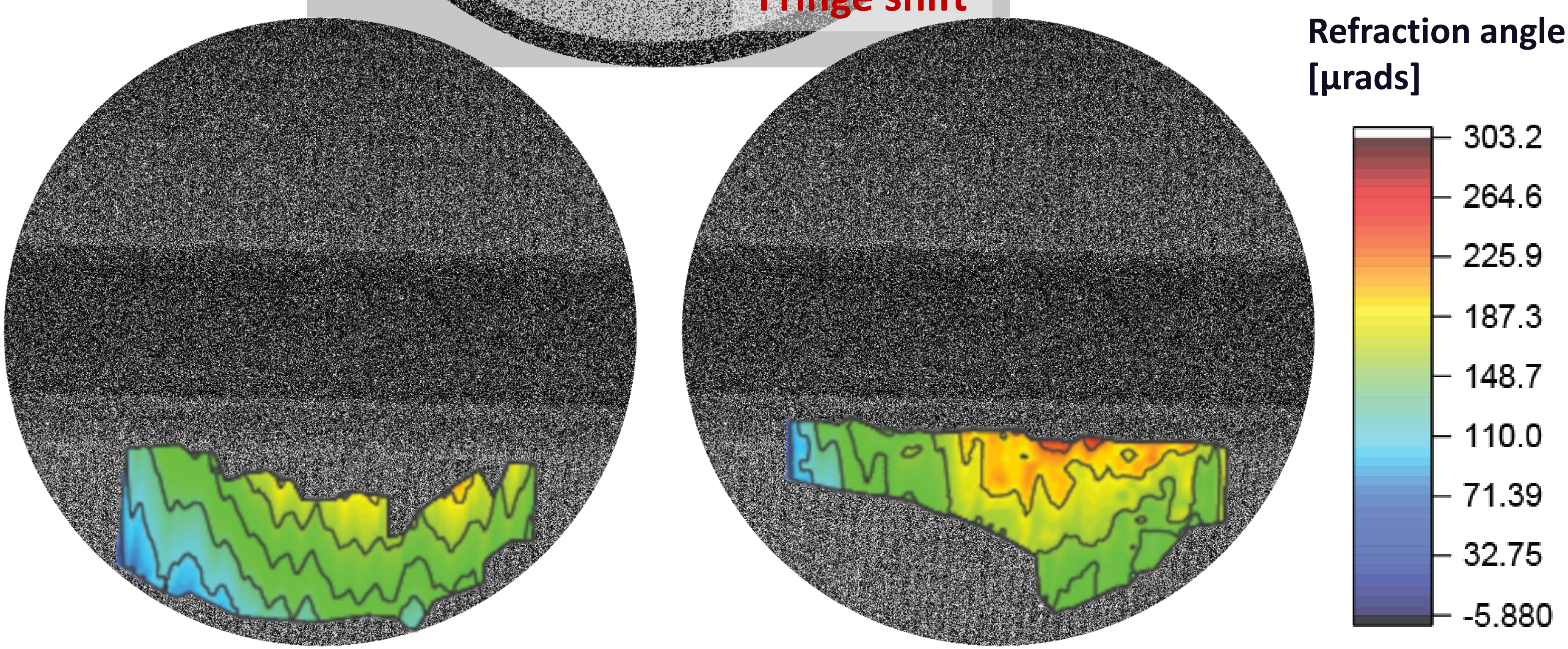

Overview of TXD diagnostics for HEDP: M. P. Valdivia, *RSI* **92** (2021)

Ablation front profiles

CER Center for Energy Research
JOHNS HOPKINS UNIVERSITY

- Low contrast and poor SNR: x-ray refraction angle mapping was preferred:

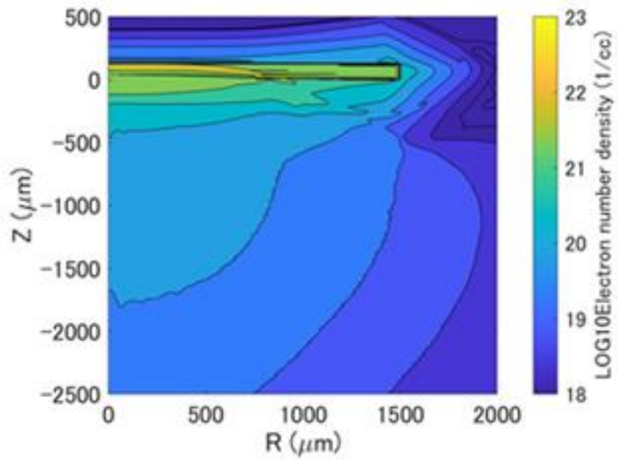

Electron density from FLASH[2]

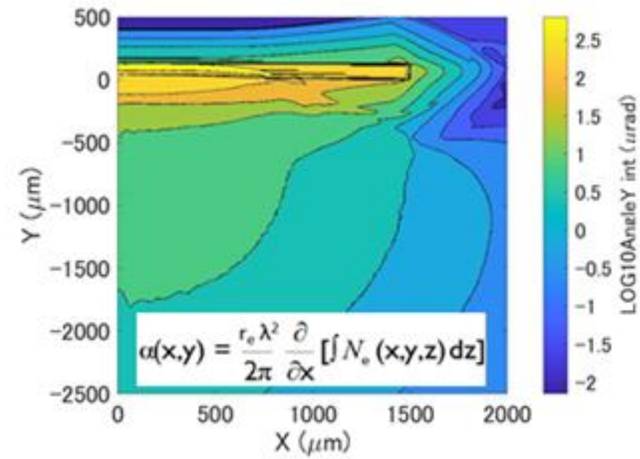

Refraction Angle[2]

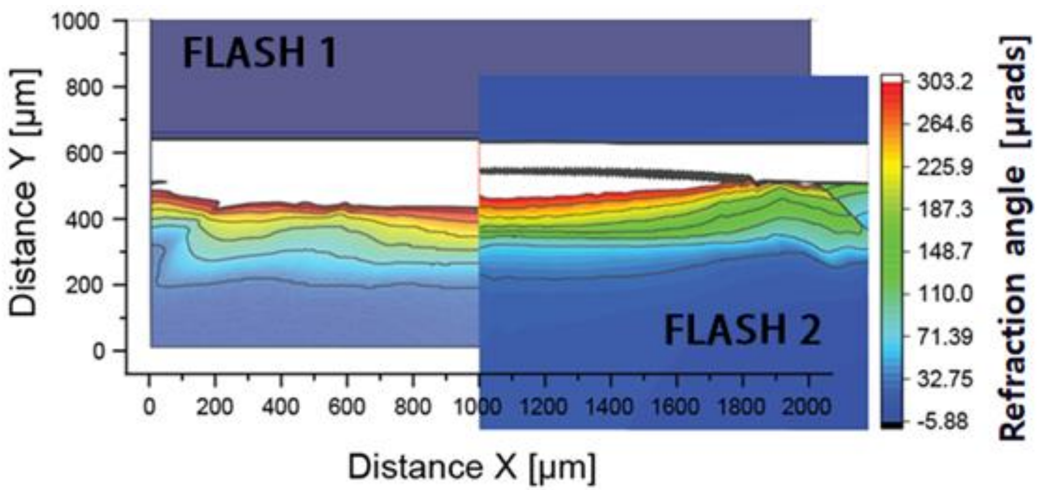

Independent FLASH simulations: Comparison between the x-ray refraction angle 2D maps obtained by post-processing the two FLASH simulations is shown.

1. Victorien Bouffetier (U. Bordeaux)
2. Kazuki Matsuo (UCSD)

*Refraction angle post-processing

Center for Energy Research

Johns Hopkins University

1) Classical approximation:

$$\alpha = \frac{r_e \lambda^2}{2\pi} \frac{\partial}{\partial x} \int n_e \, dz$$

2) Collisionless approximation:

$$\delta = \sqrt{1 - \frac{n_e}{n_c}}$$

3) Phase approximation:

$$\Delta\Phi = \frac{2\pi}{\lambda} \int \delta(x, y, z, \omega) \, dz$$

$$\delta = \frac{r_e \lambda^2 n_e}{2\pi} \qquad \alpha = \Delta\Phi \, W_{eff}$$

$$f = Z + f' + if''$$

Corrected refractive index:

$$\delta_c = \delta(Z + f')n$$

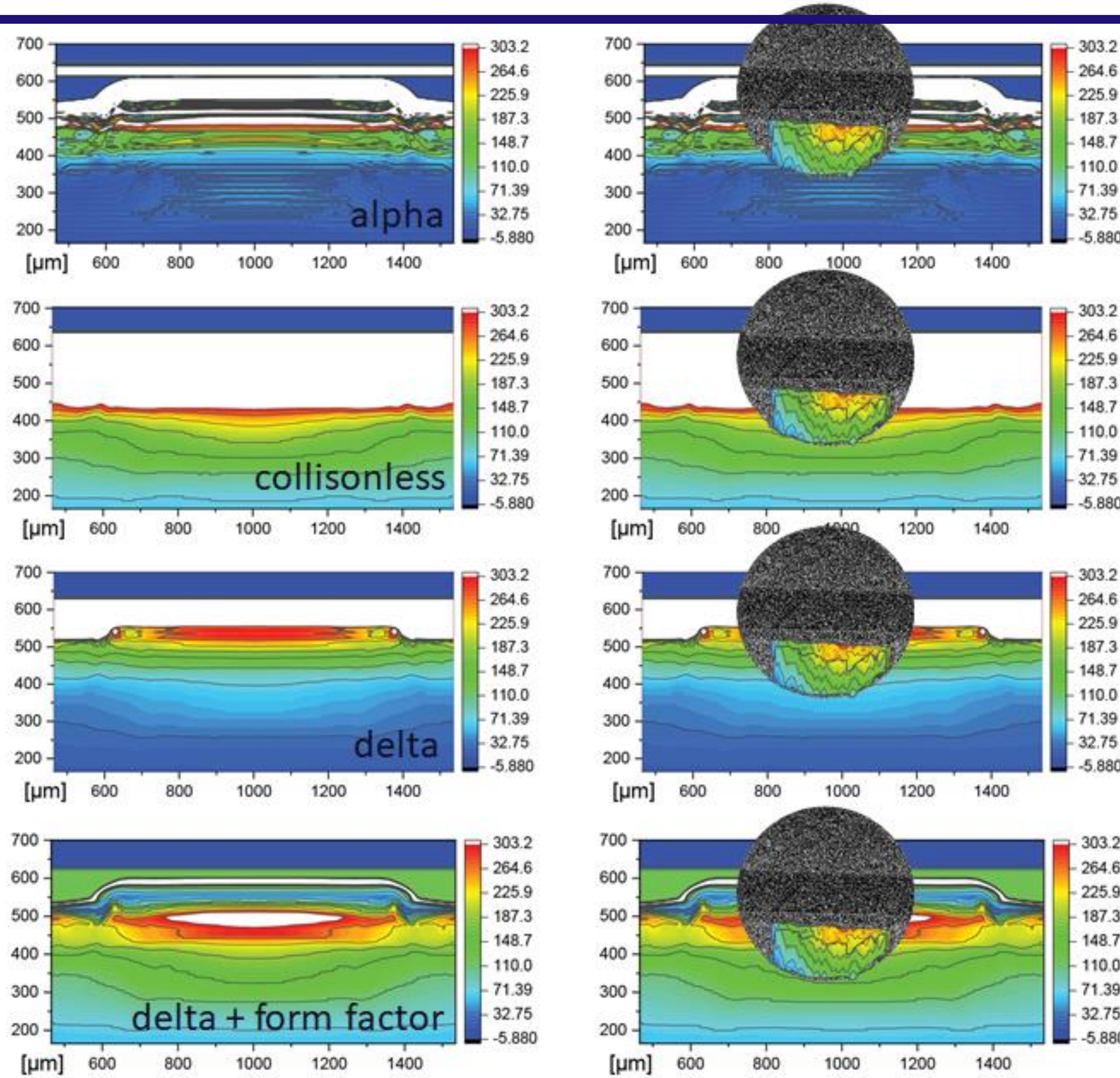

1. Victorien Bouffetier (U. Bordeaux)

CH foil ablation front: follow-up

LBS experiment (FY21): Driving beam: 150 J, 1 ns, 700 μm spot size.
Backlighter beam: 150 J, 10 ps, 120 μm spot size, Δt=0.5 ns

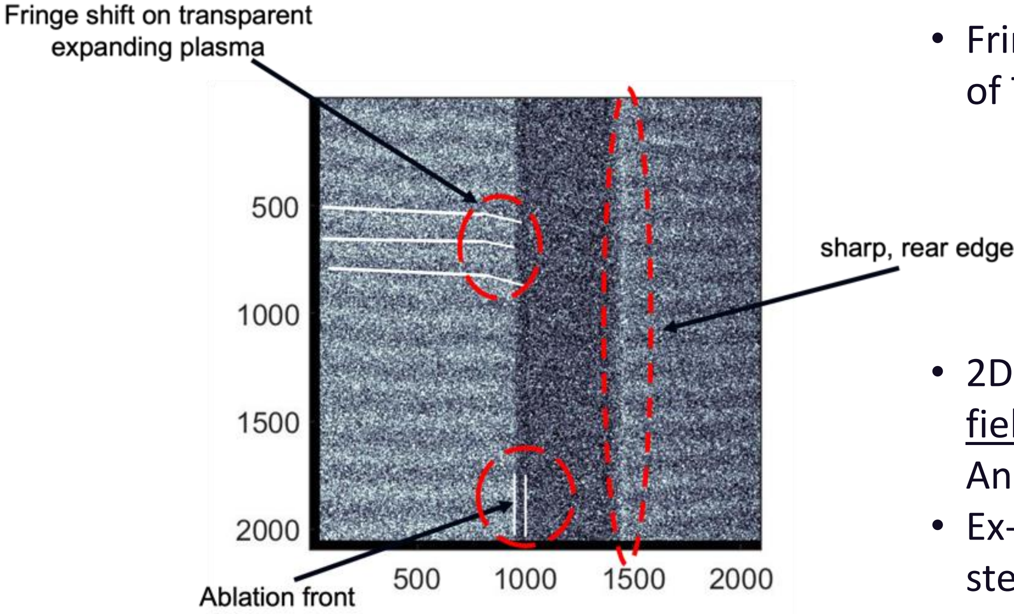

- Fringe shifts and ablation front (>10^{25} cm^{-3} limit of TXD diagnostic) observed
    - Enhanced contrast: refraction-based phase-contrast imaging (right).
- 2D maps: Phase, Transmission, and Dark-field retrieved with Talbot Interferometry Analyzer (TIA) code.
- Ex-situ reference Moire image from phase-stepping methods (on-site x-ray station).

- Once backlighter optimization is achieved: higher Moire fringe contrast will enable improved electron density, scatter, and elemental composition diagnostic capabilities for HEDP.
- Further enhancement expected from: Monochromatic TXD diagnostics
- Advanced methods: TIA code and ex-situ reference images obtained through Phase-Stepping.

***TIA:** G. Perez-Callejo, *Applied Optics* **Accepted** (2022)

*Phase-stepping ex-situ reference

- Demonstration of reference Moire image acquisition through phase-stepping: accurate Phase, Transmission, and Dark-field retrieval.

  * No additional laser shot required to obtain a reference image.

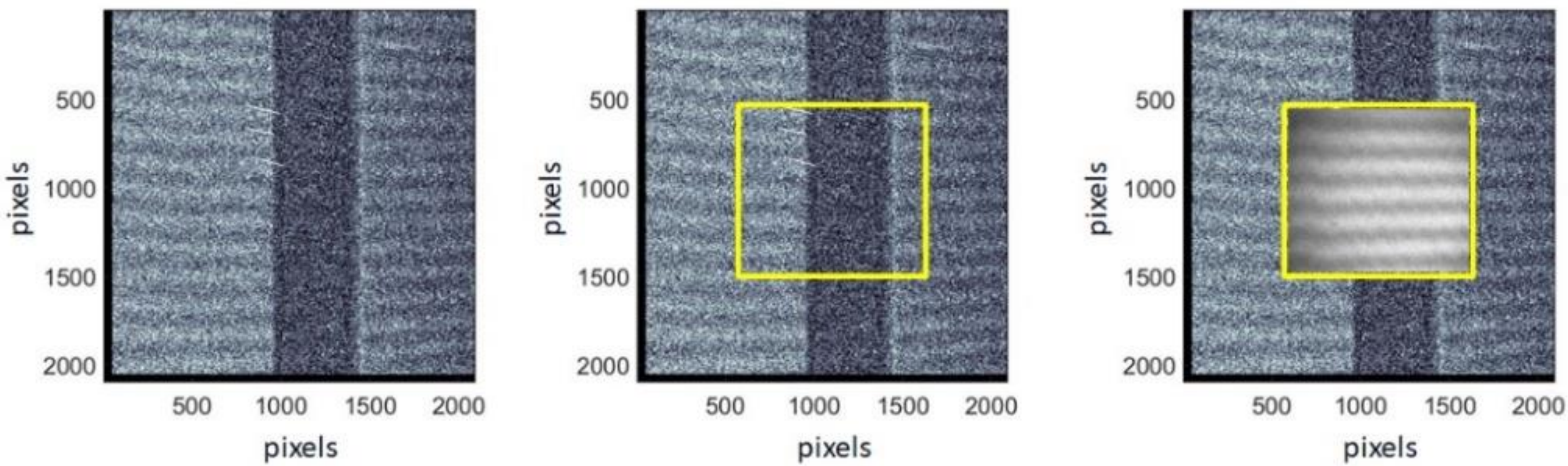

- Moire images: yellow FOV from x-ray alignment station at LLE
- Last panel: One Phase-Stepping image (best correlated)

*Dark-Field images from TXD

Transmission

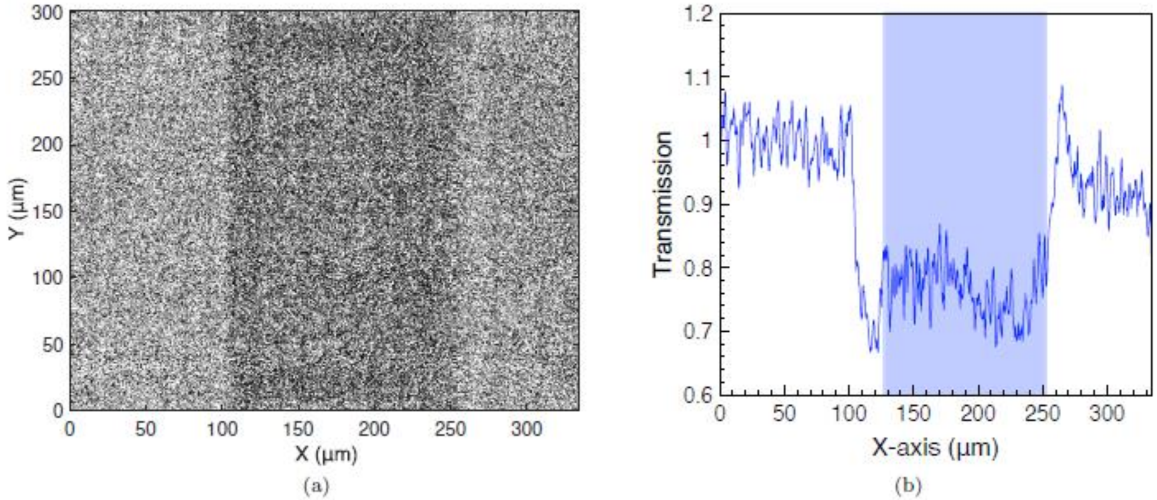

Dark-Field

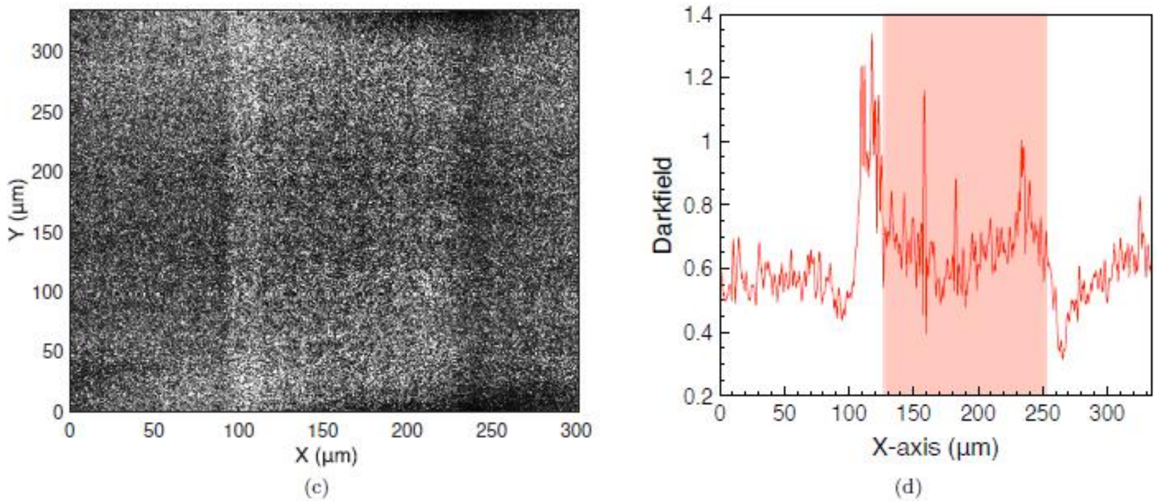

Dark-Field imaging of irradiated foils: G. Perez-Callejo, *manuscript in preparation*

Monochromatic TXD

Goal: Increase Moire contrast through x-ray backlighter improvement. Based on results from previous Omega EP campaigns, monochromatic x-ray sources will be beneficial

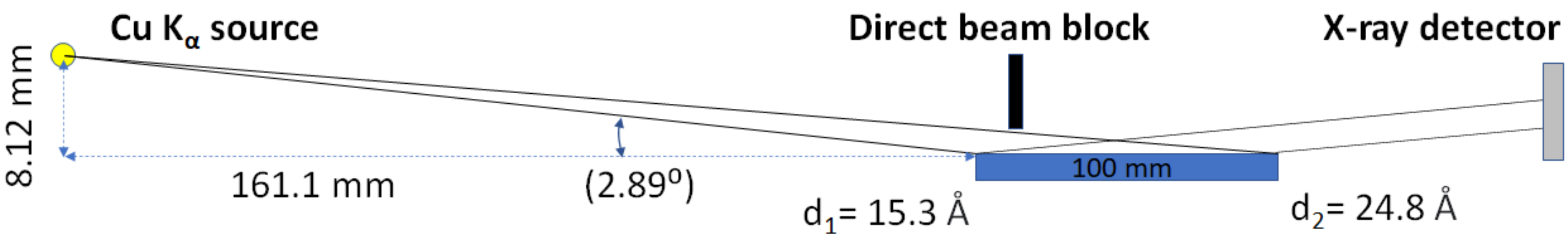

Test with Cu x-ray tube (continuous source)

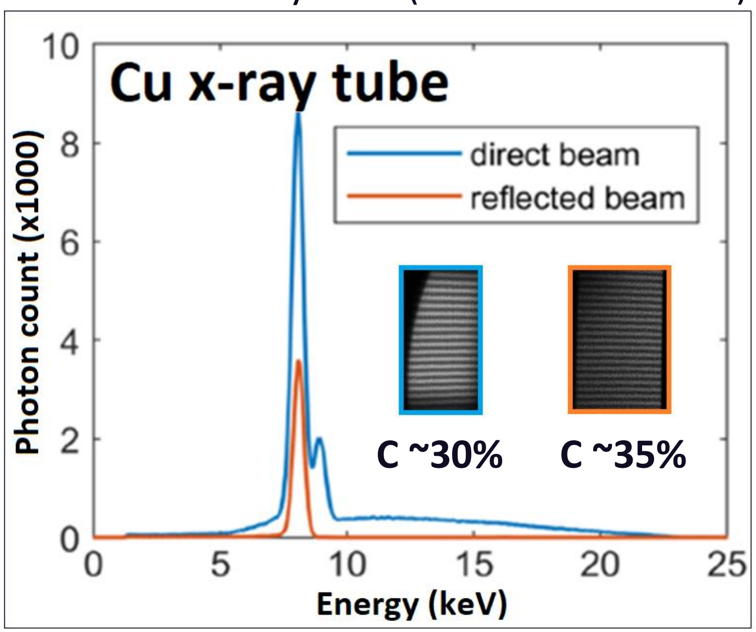

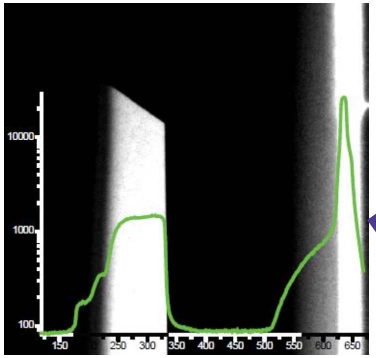

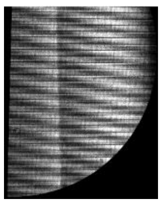

8 keV reflection

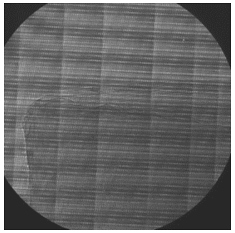

Broad spectrum

Monochromatic MTW (FY21)

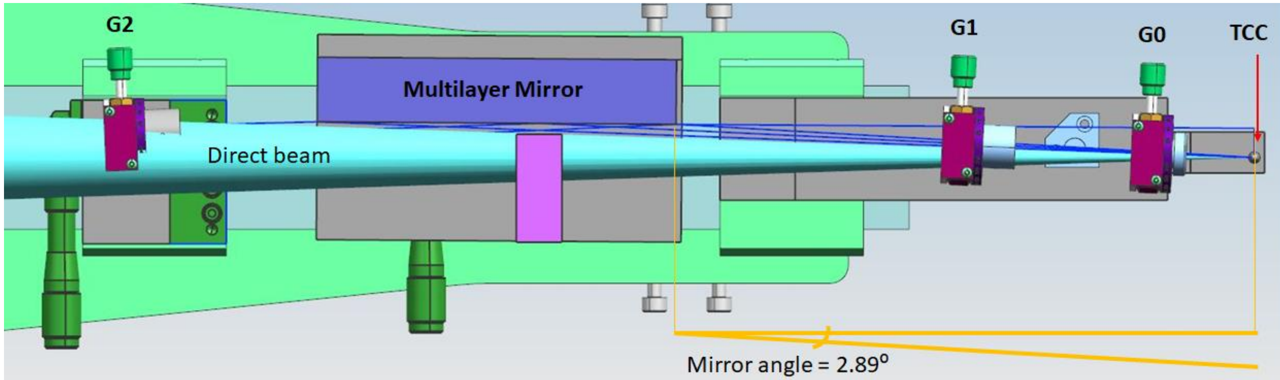

X-ray station images:

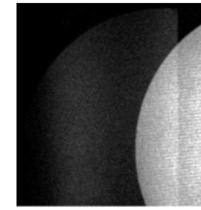

CCD: Direct beam and reflection

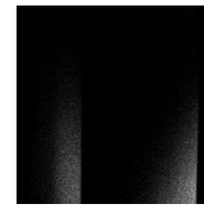

… beam block added

First tests on MTW (FY21): Very low x-ray flux on CCD detector:

- New source gratings have lower transmission (fabrication)
- Multi-Layer mirror: reflectivity of ~25% (of 8 keV energy)
- Mirror alignment ***extremely*** sensitive (reflection angle)

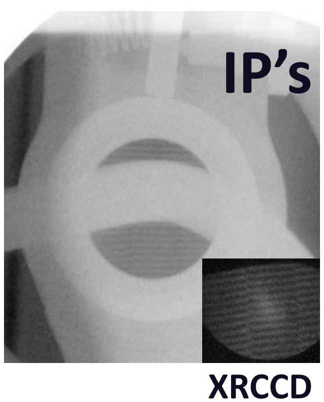

Contrast: X-ray CCD ~20%
Image Plates ~4%

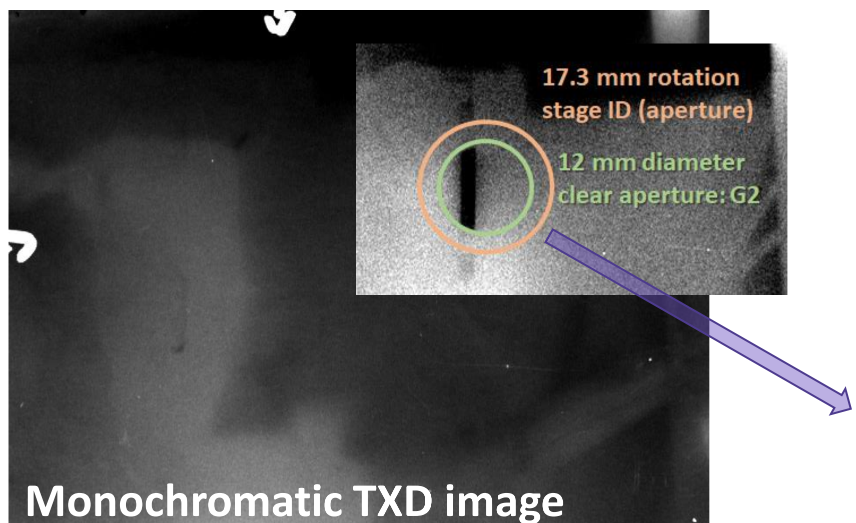

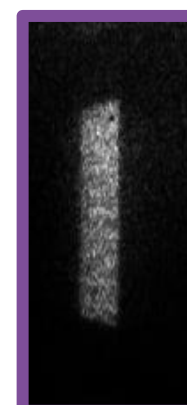

Contrast: ~8%

Monochromatic EP-TXD

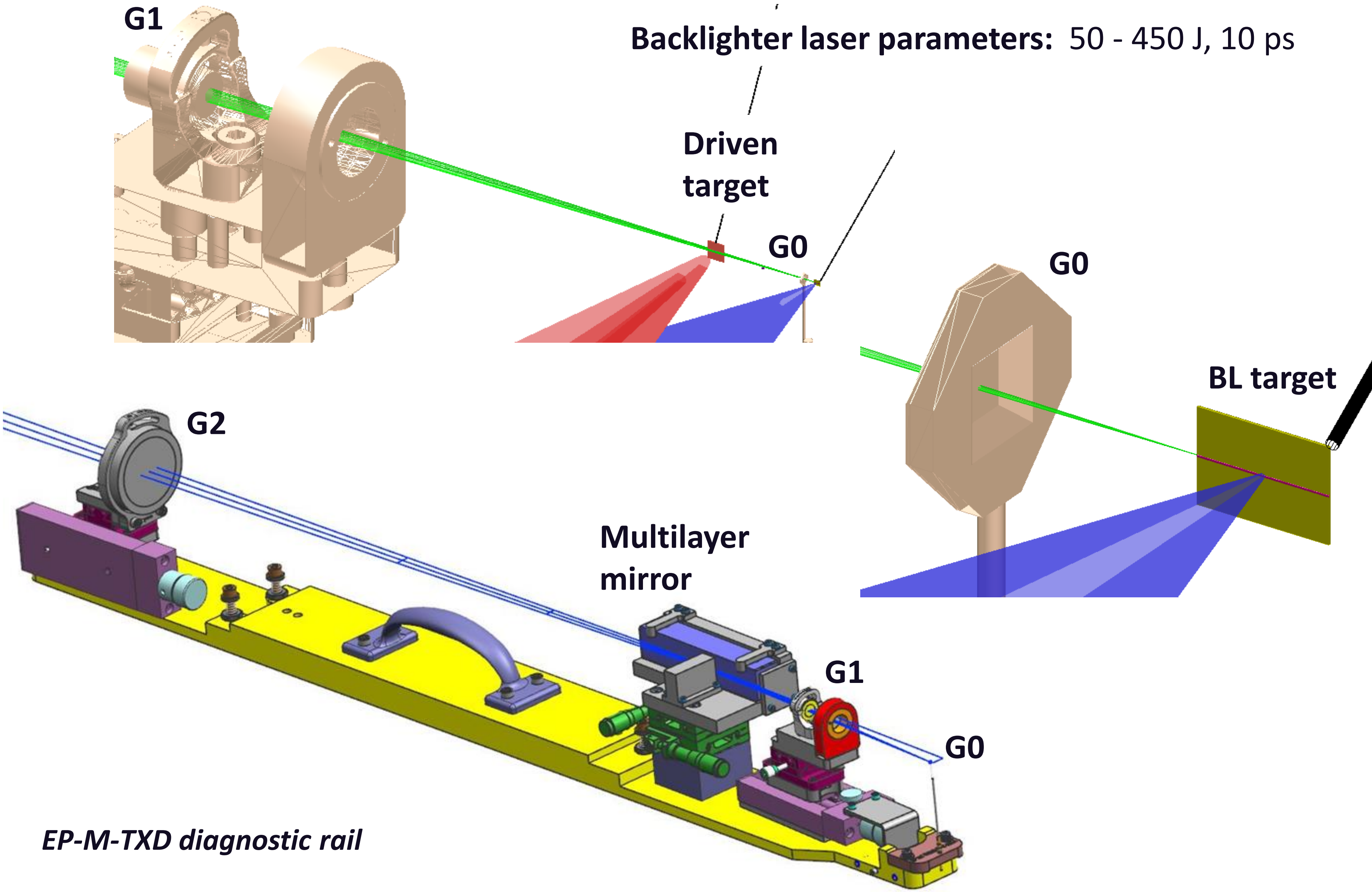

EP-M-TXD diagnostic rail

EP-M-TXD campaign (FY21)

*No driven shots

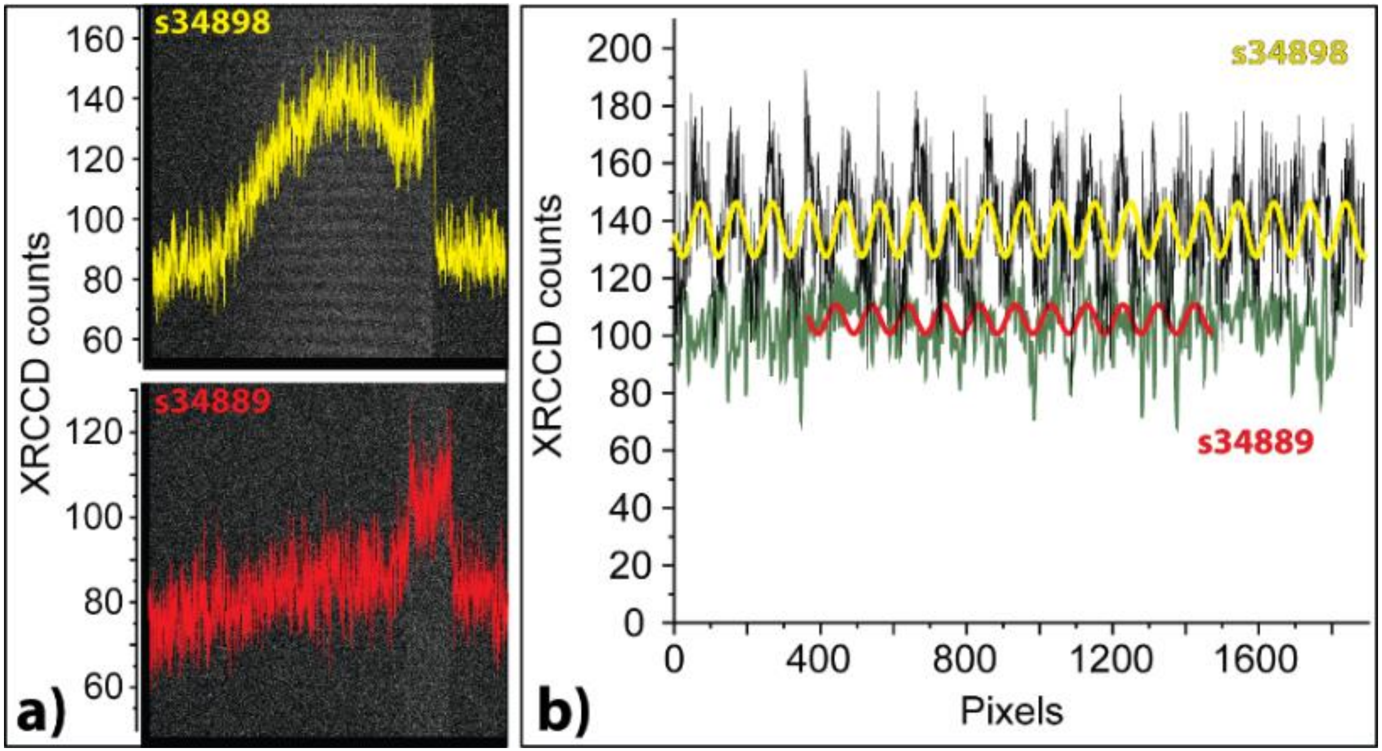

- Diagnostic performance compromised: low flux at detector (~50 photons per pixel vs. >300 expected from previous campaigns considering ~25% mirror reflectivity)
- Backlighter: Edge-on Cu foil -> <u>Best flux for ~5° rotation</u>
- New source grating fabrication methods reduced transmission by a factor of ~3-4x

Monochromatic TXD: MTW FY22

Changes from previous campaign:

- Old source gratings (x4)
- XRCCD and G0 protective filter (x2)
- TXD rail alignment:
  Dedicated XR station setup for MTW

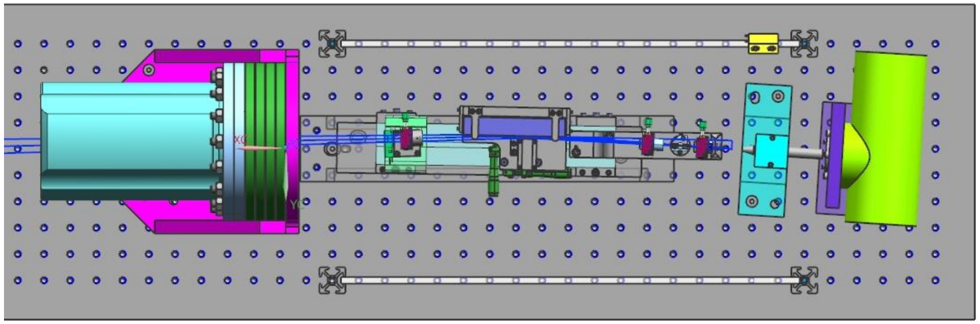

Monochromatic TXD: MTW FY22

CER Center for Energy Research
Johns Hopkins University

Changes from previous campaign:

- Old source gratings (x4)
- XRCCD and G0 protective filter (x2)
- TXD rail alignment:
  Dedicated XR station setup for MTW

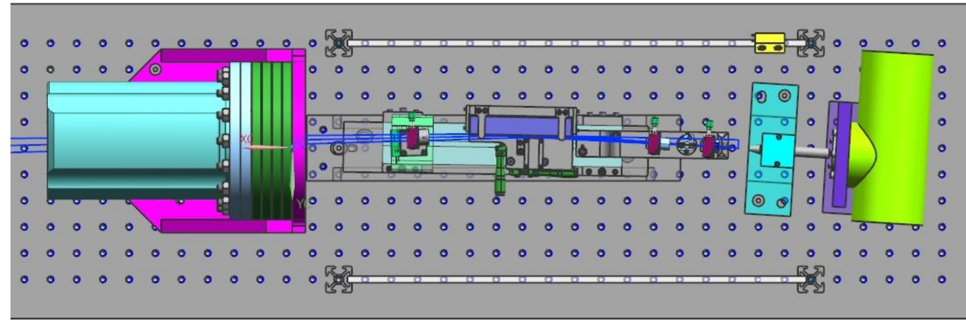

X-ray alignment images:
- Continuous x-ray tube (Cu anode)

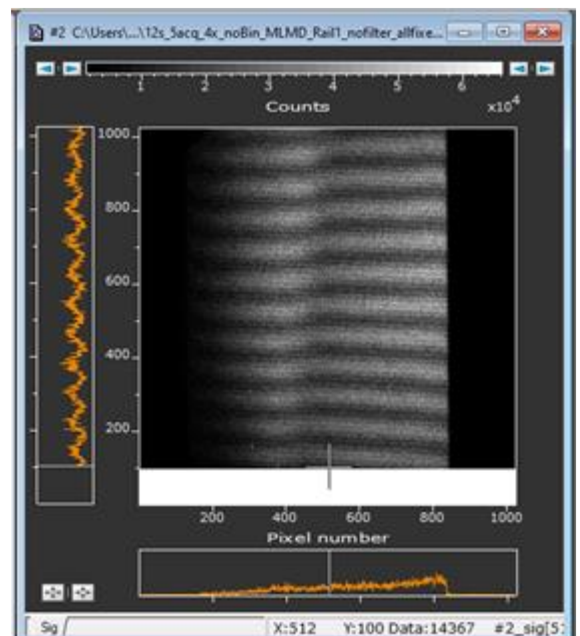

Monochromatic TXD: MTW FY22

Changes from previous campaign:

- Old source gratings (x4)
- XRCCD and G0 protective filter (x2)
- TXD rail alignment:
  Dedicated XR station setup for MTW

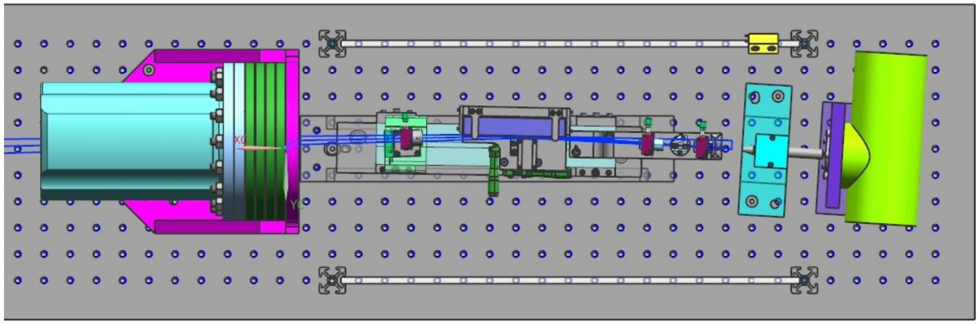

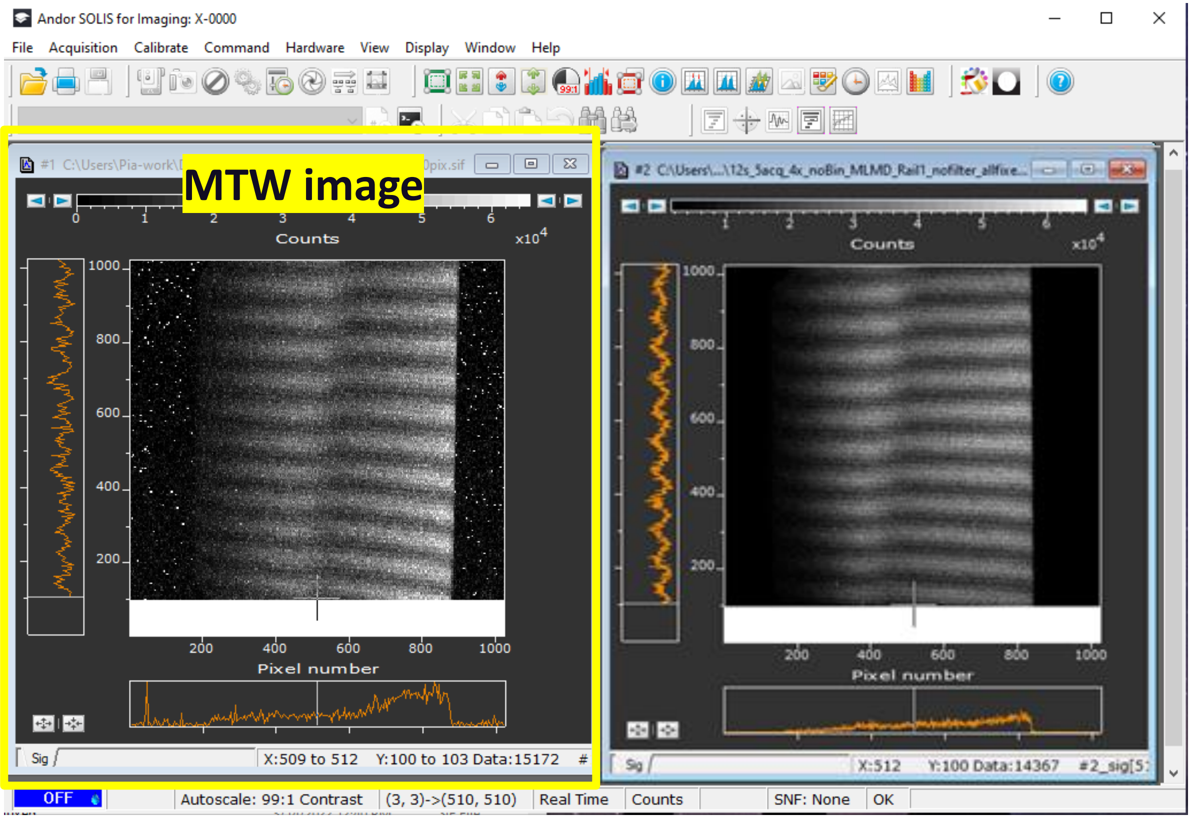

M-TXD: MTW backlighters

Center for Energy Research

Johns Hopkins University

Systematic studies: Rail alignment, target, laser pulse length and energy

Intensity: 2 $\times 10^{14}$ – 1 $\times 10^{15}$ W/cm^2

1) Rail alignment (27 J, 20 ps, ~8 $\times 10^{14}$ W/cm^2):

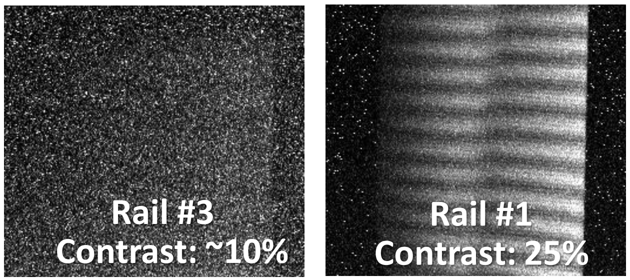

Pulse length: 10, 20, ~60-80 ps

Target defocusing: laser spot size (x-ray LOS change)

2) Target type (36 J, 57 ps, ~4 $\times 10^{14}$ W/cm^2):

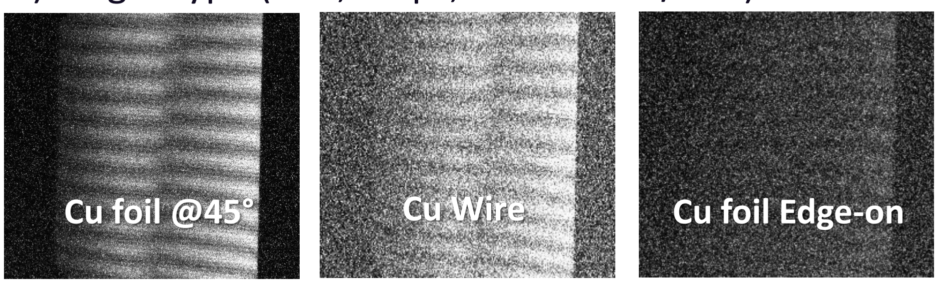

Targets:

- Foils w/ 3D printed stalks: less background
- Cu wires (CH backed): old stalks
- Orientation (~45° to Edge-on): Alignment

3) Cu foil orientation (29 J, 84 ps, ~3 $\times 10^{14}$ W/cm^2):

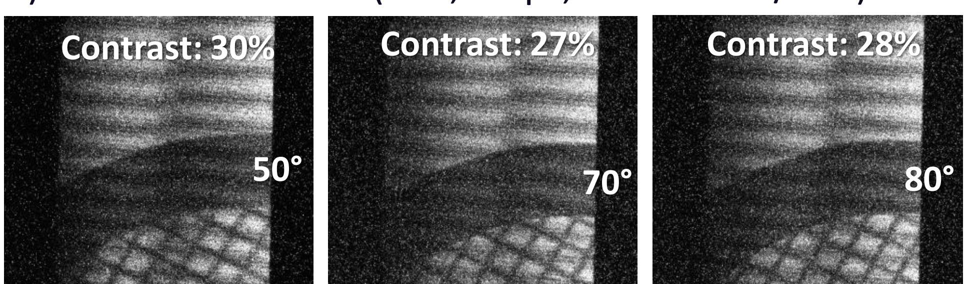

Spatial resolution:

- ~10 µm for 50° foil
- ~8 µm for 70° foil
- ~6 µm for 80° foil

* Detector limit: 5.5 µm

M-TXD: MTW backlighters

Retrieval: Phase, Transmission, and Dark-Field

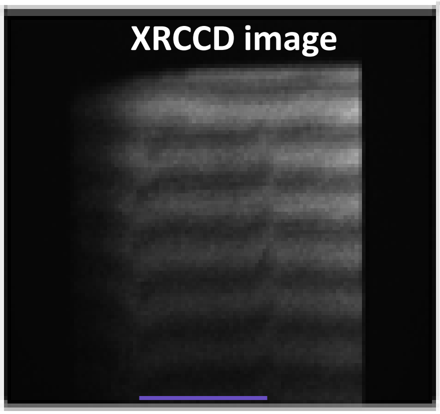

PMMA rod: 750 µm diam.

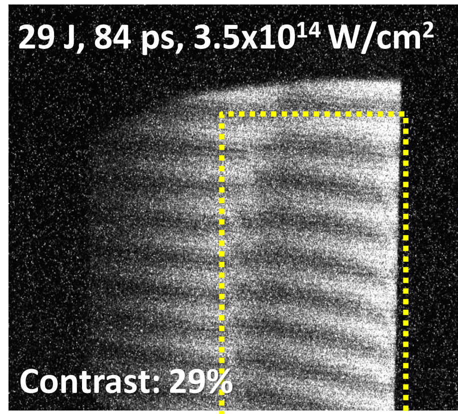

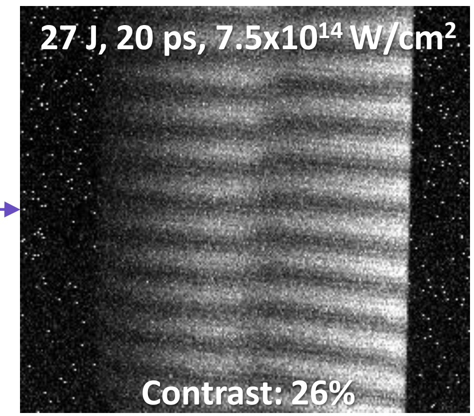

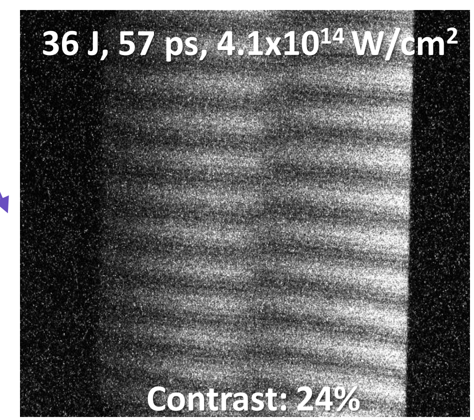

Reference image:

- Not available from experiment or Phase-Stepping
- MTW reference with different BL specs:
  - TIA code: backlighter profile feature
  - Correlation methods to match fringes

Pending data analysis:

SNR, Flux comparison, Spectra, Conversion efficiency, Resolution… related to laser intensity, targets, etc

Future experiments (FY22Q4)

NLUF:
With Dan Haberberger, Alex Shvydky (LLE)

Goal:
Map electron density gradient of irradiated-shell with TXD

- Experimental results will be compared with simulated FLASH images
- TIA code will be benchmarked: post-processed images with experimental results and XWFP simulations using FLASH n_e profiles

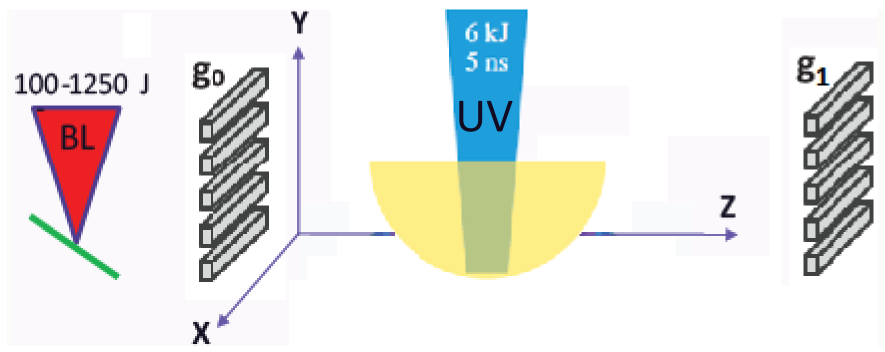

Figure 3: CH shell (yellow) driven by long-pulse beams. Cu foil driven by short-pulse backlighter for TLX interferometry.

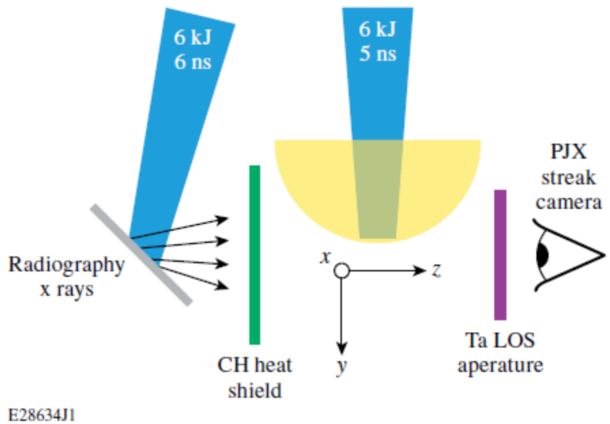

PHYSICAL REVIEW LETTERS **123**, 235001 (2019)

Future experiments (FY22Q4)

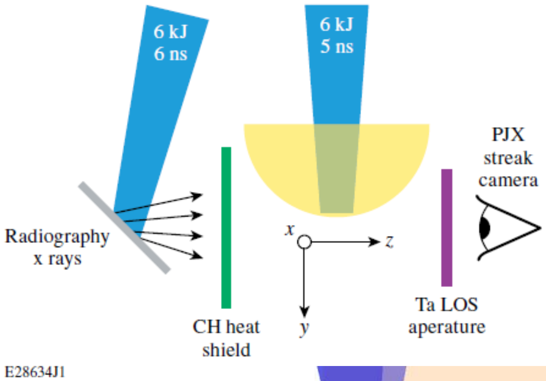

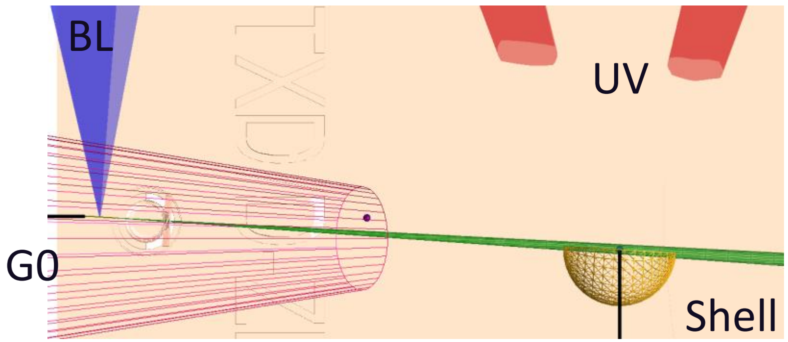

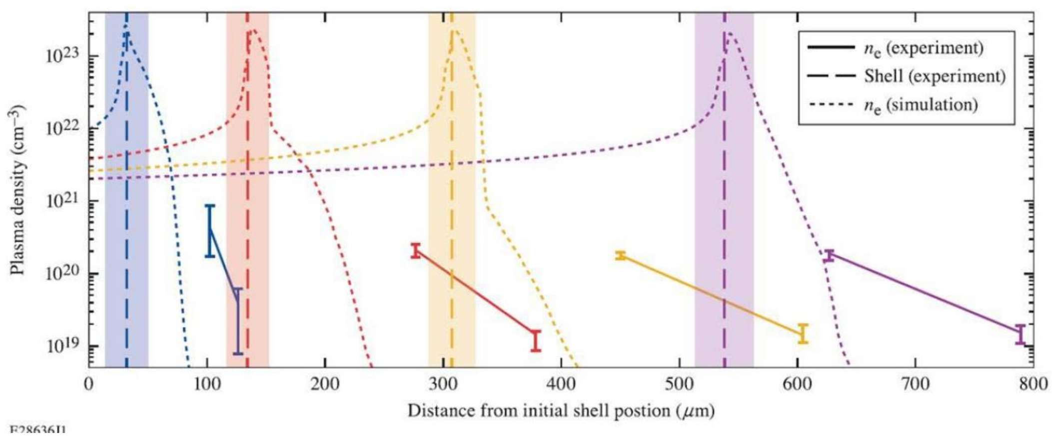

PHYSICAL REVIEW LETTERS 123, 235001 (2019)

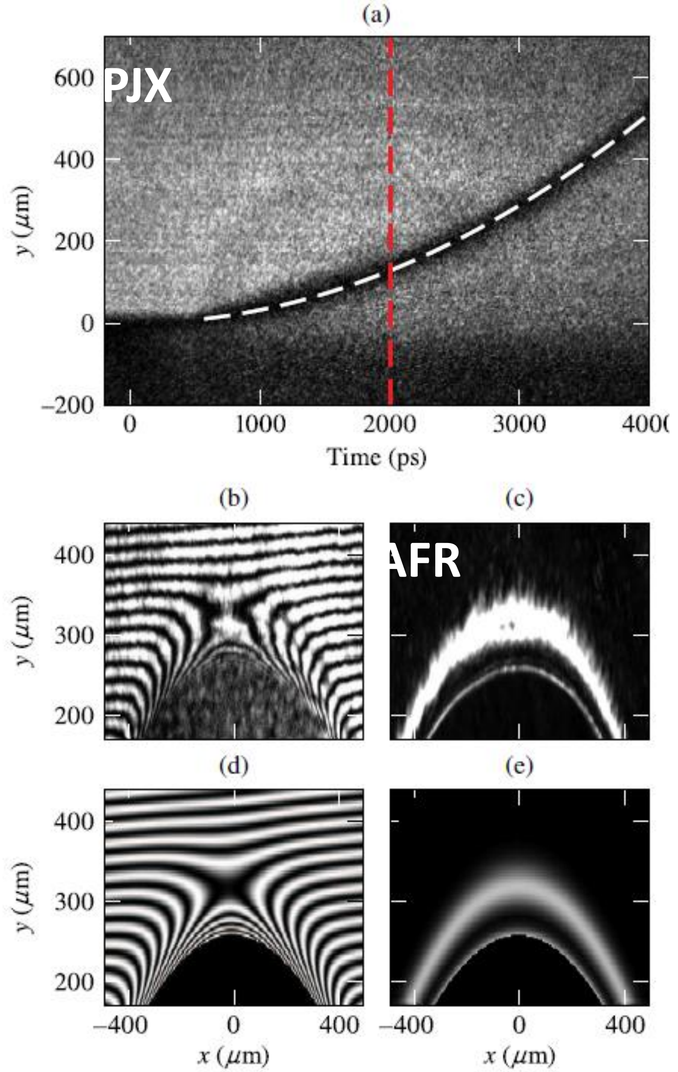

Summary

TXD capabilities:

- Areal n_e gradients detection through **refraction** (and **attenuation**)
- Micro-turbulence and material mixing through **Z-average**
- Hydrodynamic instability through **scatter** (Dark-Field)
- Enabled by new methods and algorithms: TIA code, Phase-Stepping, etc

TXD tested in HED environment:

- **MTW**
- *LULI
- *ECLIPSE
- **OMEGA-EP**
- *XFEL: SACLA
- *Pulsed-Power (x-pinch x-ray sources): Llampudken and GenASIS

*Not shown

Back-up slides

TXD tested in HED environment:

- XFEL: SACLA
- TIA code:
  - SACLA analysis
  - Code capabilities
- Future experiments: LCLS-MEC (XFEL)
  - Foams: Shock dynamics
- Pulsed-Power
  - Motivation: MagLIF
  - GenASIS results

XFEL: XPCI with TXD

Monochromatic TXD with XFEL beam at SACLA: metallic foils irradiated.

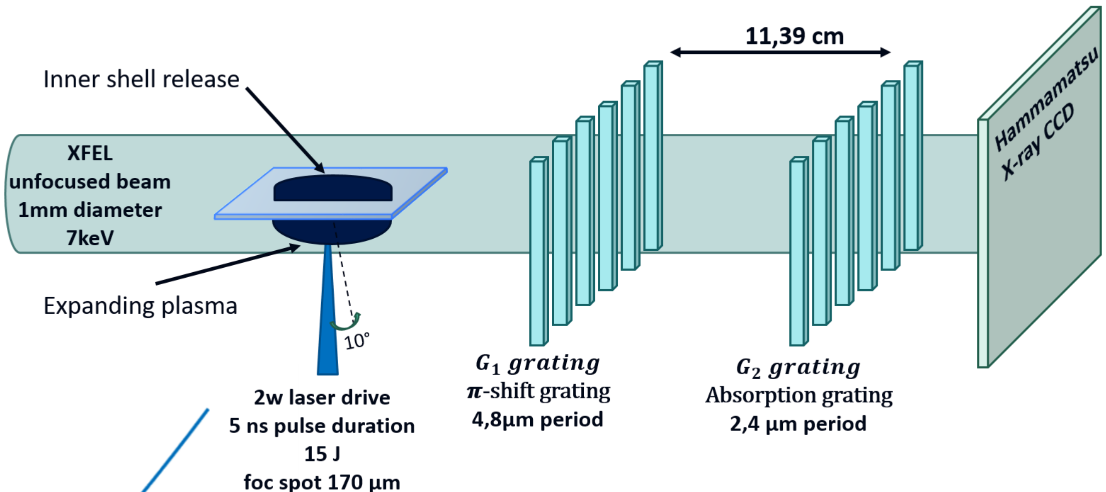

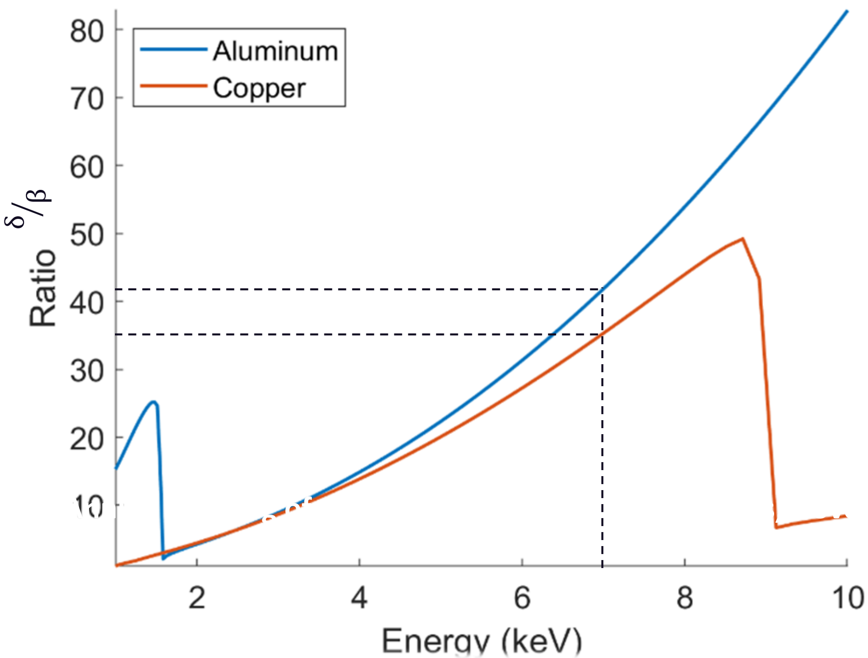

- Phase, attenuation, and dark-field images retrieved using the TIA software: resolution ~11 µm but can be optimized to ~2 µm

- Compared to propagative X-ray Phase Contrast Imaging (XPCI) method, no assumption is made to retrieve transmission and phase images, enabling an absolute measurement of the refractive index.

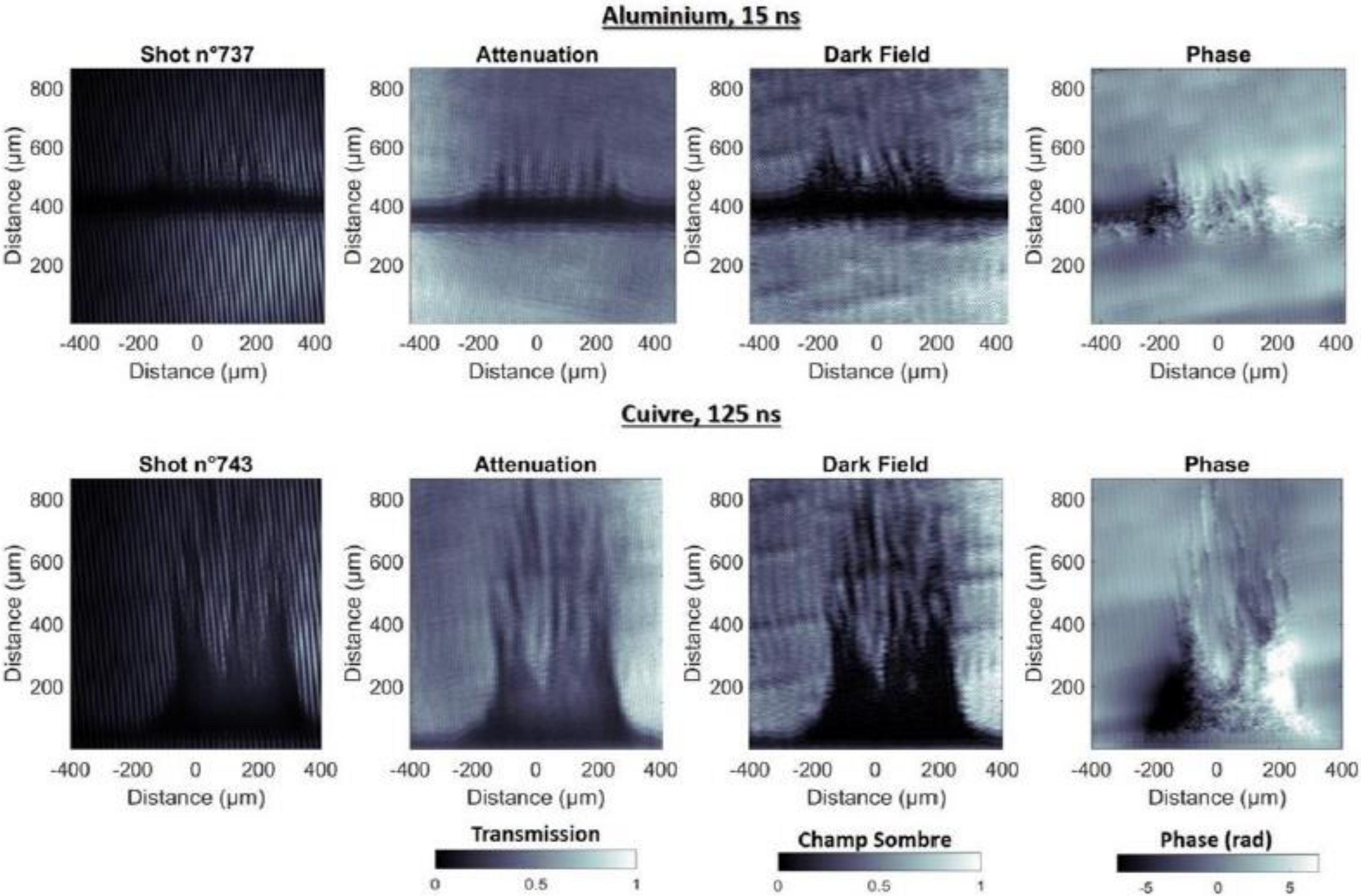

Moire images delivered a ~50% fringe contrast using a high Talbot order (m=7). Two foil targets probed at different times are shown. TIA code used to retrieve attenuation, dark-field, and phase images. There is a clear distinction between a mid-Z (Al) and high-Z (Cu) material.

Advanced retrieval methods: TIA§

Cu foil irradiated by 5 ns laser pulse (~10^{13} W/cm^2) at SACLA. Attenuation, phase, and dark-field maps retrieved through TIA code. Initial results (top) improved through implementation of additional algorithm capabilities (bottom).

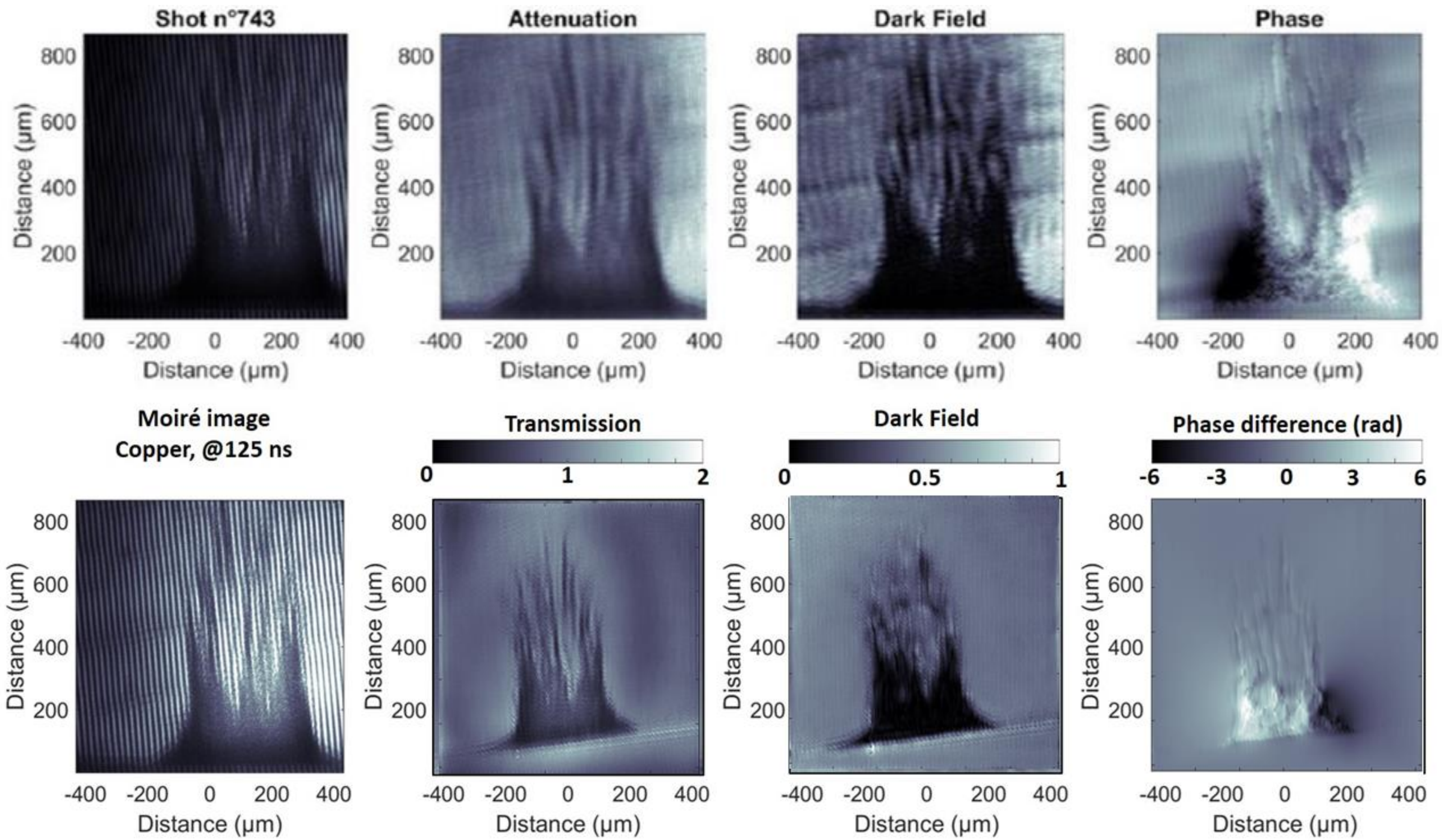

§ **Talbot Interferometry Analyzer:** G. Perez-Callejo, *Applied Optics*, accepted (2022)

Advanced retrieval methods: TIA§

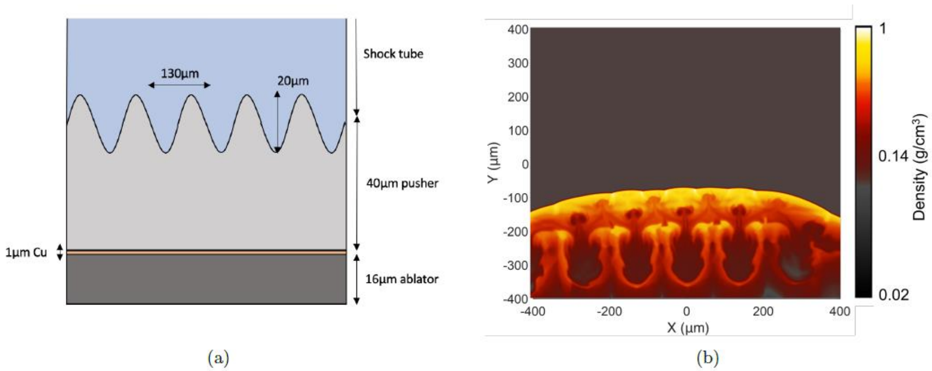

FIG. 4: 4a Original target design and 4b density map at 30 ns for the example simulation. The density figure is presented in logarithmic scale to show the different regions of the expanding plasma.

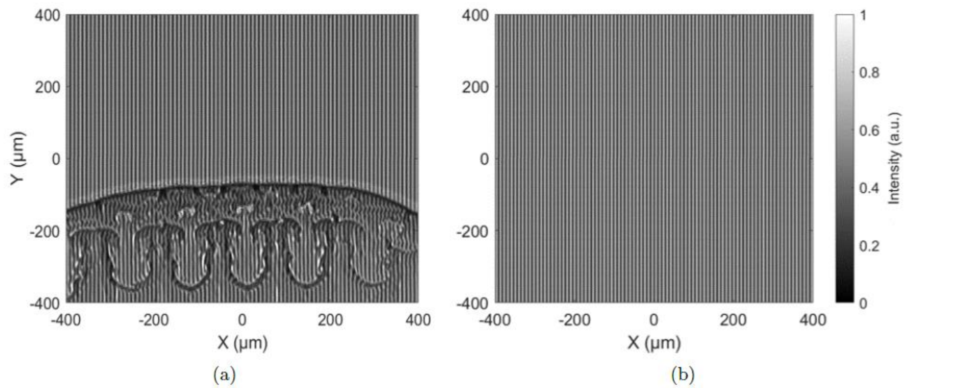

FIG. 5: Interferometry (5a) and reference (5b) images generated by TIA for the example case shown in Figure 4b.

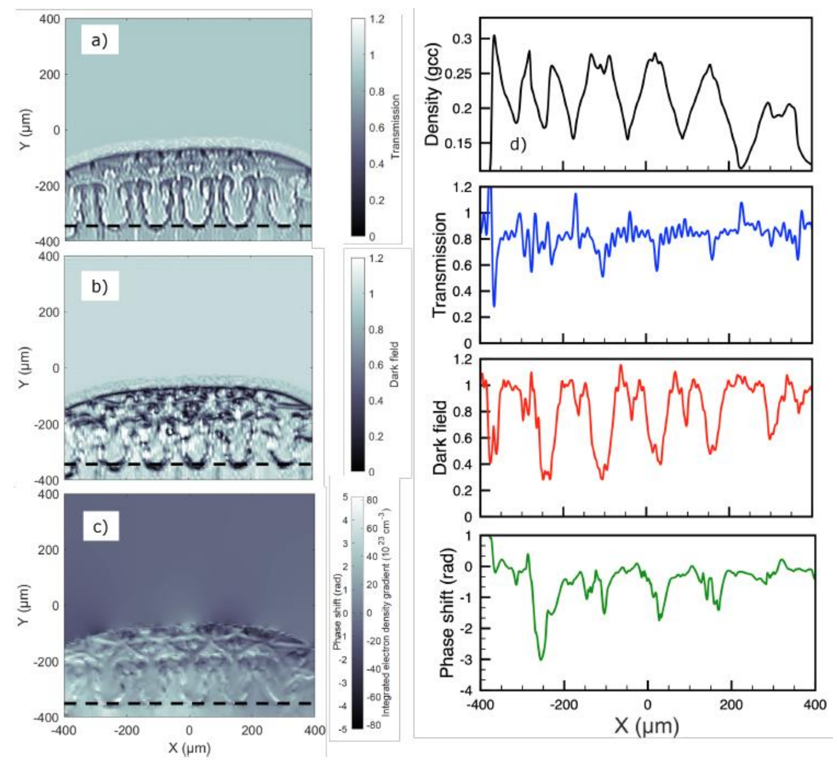

FIG. 6: Results from the example case. (a) Transmission image, (b) dark field image and (c) phase shift. The colorbars and contrast have been adjusted so that the features of the plasma can be easily observed in all images. An additional scale has been added to the phase shift figure, indicating the equivalent values of the integrated electron density gradient $\left(\vec{\nabla}(n_e z)\right)$ that can be measured with this system. Panel (d) shows 20 μm-wide horizontal lineouts through $y = -360$ μm, together with the corresponding density lineout from the hydrodynamic simulation in Figure 4b, for comparison. The horizontal dashed lines have been included for guidance. Note how the transmission in this case is very low compared with the dark field features, showing the advantages of using interferometry with respect to X-ray radiography in these cases.

§ Talbot Interferometry Analyzer: G. Perez-Callejo, *Applied Optics*, accepted (2022)

Future experiments: LCLS-MEC

Center for Energy Research

Johns Hopkins University

Shock studies: Foam targets

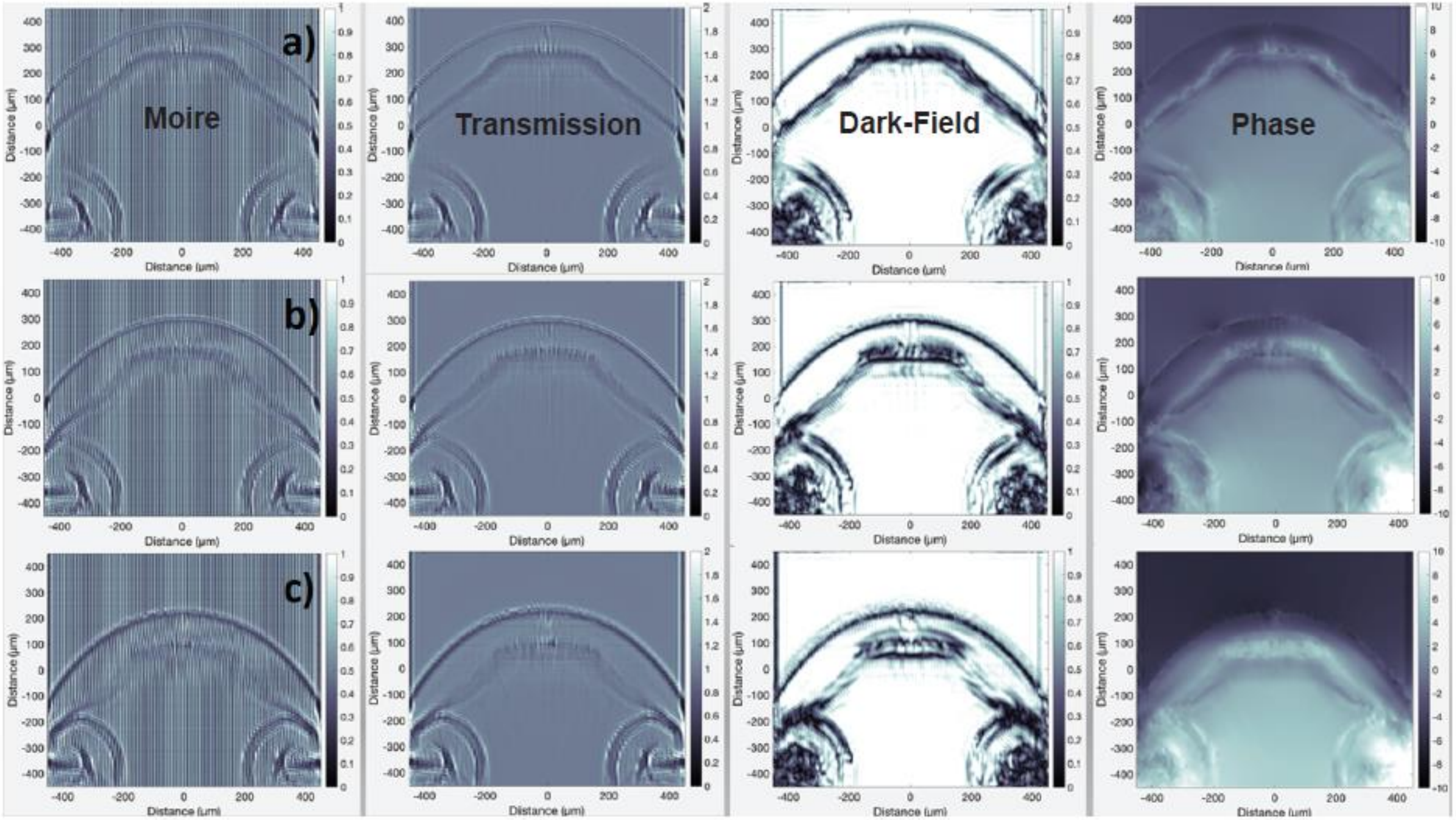

Figure 2: **Shocked foam images.** Synthetic Moiré, transmission, dark-field, and phase images of: a) 20 mg/cc, b) 50 mg/cc, and c) 100 mg/cc foams driven by a 60 J, 10 ns, 400 μm spot size laser pulse.

LCLS-MEC: Shock dynamics

Center for Energy Research

Johns Hopkins University

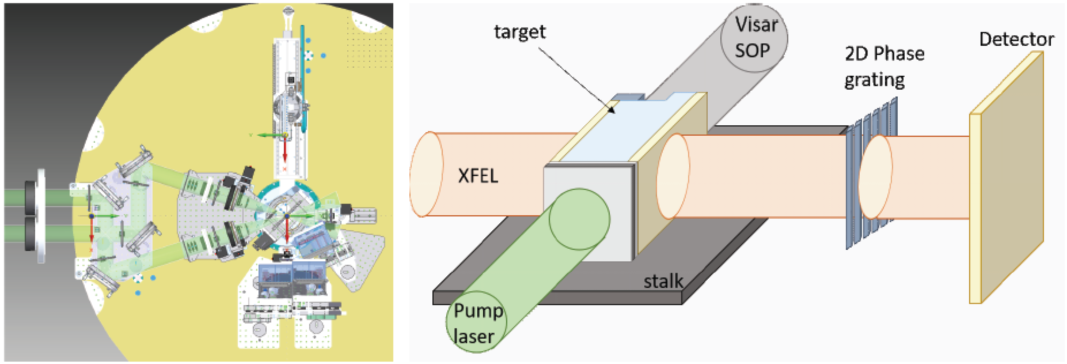

Figure 3: **MEC chamber and experiment schematic.** 3D model of the MEC vacuum chamber (left). Experimental setup for shock studies including beams, target, and diagnostics.

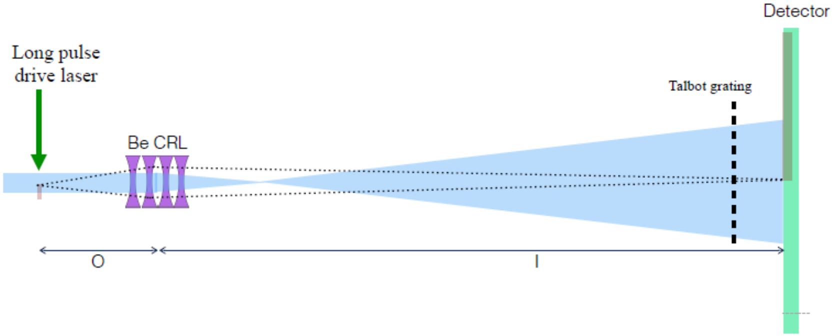

Figure 5: **Experimental setup.** The MEC long pulse laser drives a shock wave in the sample. LCLS laser beam illuminates the foam. Behind the sample, a stack of Be lenses images the sample onto a scintillator based X-ray microscope with geometric magnification of ~20X. The Talbot grating is placed at the appropriate Talbot distance in front of the camera for phase measurements.

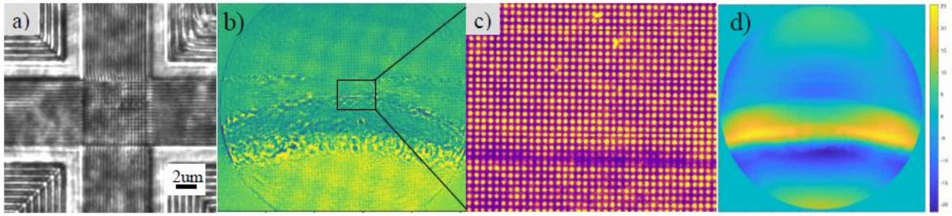

Figure 6: **Previous results of Talbot Imaging at MEC** a) Image of a resolution target. The thin lines in the center have a width of 200 nm. b) Talbot image of a shock wave traveling through a Si sample and c) closeup around the plastic shock front, that shows the 3D Talbot image. d) Reconstructed phase of image b).

Pulsed-power motivation

Refraction Enhancement

- Mid-intensity modulation of phase-curve (quarter-period) enhances contrast, especially sharp n_e gradients and interphases.
- MagLIF: experiments with ~10 μm liner features of 100 μm order: $\mathbf{n_e = \sim 10^{23\text{-}24}\ cm^{-3}}$.
- Ranges optimized considering angular refraction expected from plasma ROI, through: design energy, grating bar period, and object position.

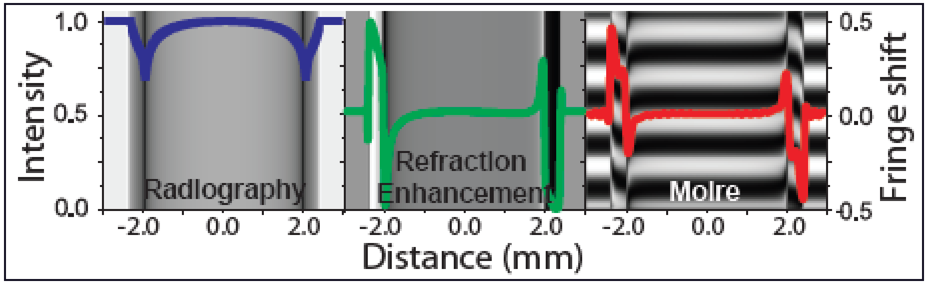

Figure 7: Simulated H filled (ρ=0.167 g/cm³) Be liner (OD=1.5 mm, ID=1 mm) with thin Al layer (5 μm) probed @8 keV.

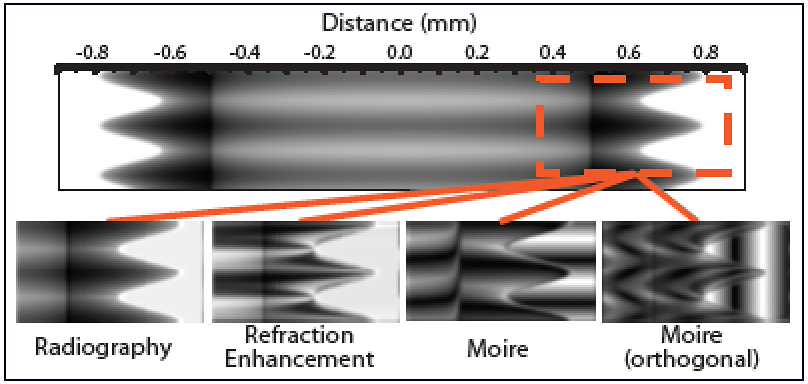

Figure 8: Simulation of hollow plastic cylinder (OD = 350 μm, ID = 246 μm) with sinusoidal axi-symmetrical profile of 100 μm amplitude and ~150 μm period.

X-pinch x-ray backlighter

Center for Energy Research

Johns Hopkins University

Motivation: Image HED object in the pulsed power environment

- X-pinches: x-ray sources for point projection radiography, lithography, diffraction, and absorption spectroscopy

- Three types tested on GenASIS current driver (200 kA, 150 ns)

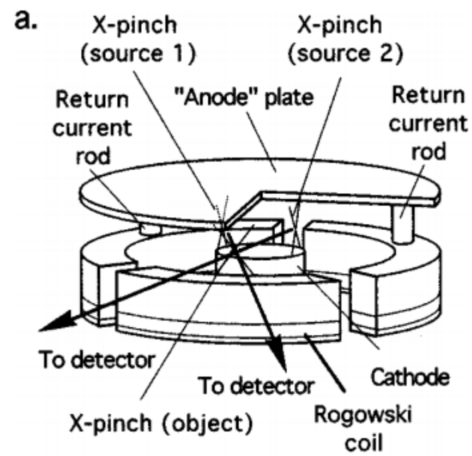

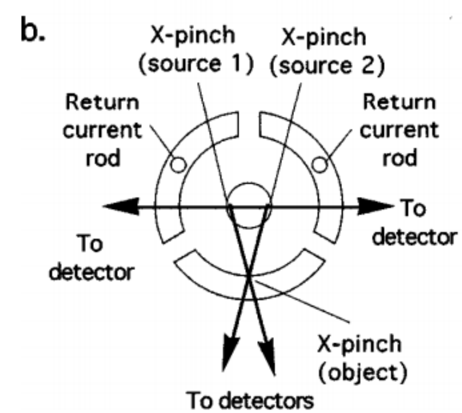

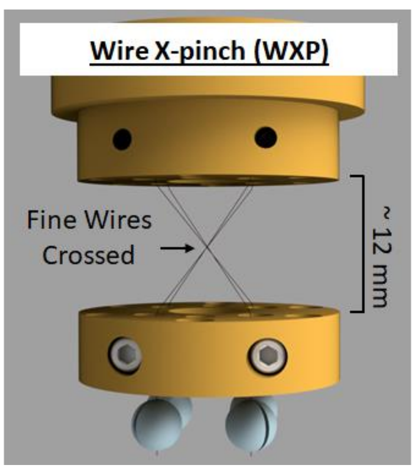

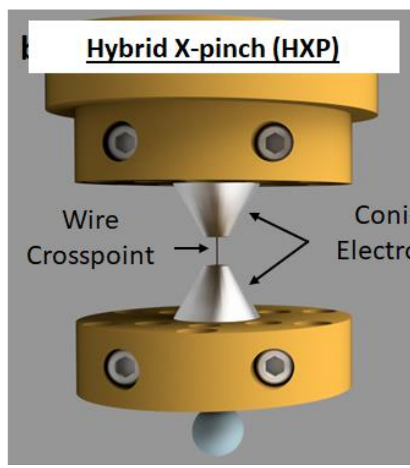

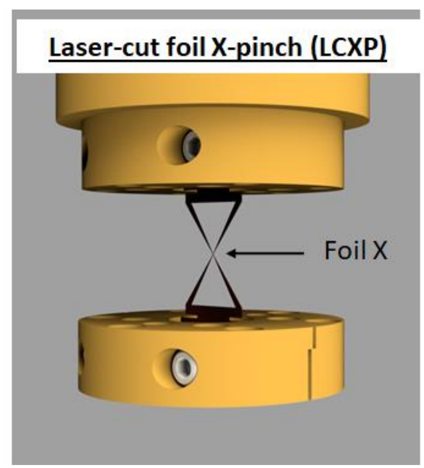

Laser-cut: GenASIS

- Laser-cut x-pinches: Best spatial resolution to date out of all TXD adaptations
- Highly reproducible, <5 µm Cu k-alpha emission within contrast curve. High contrast using image plate detectors

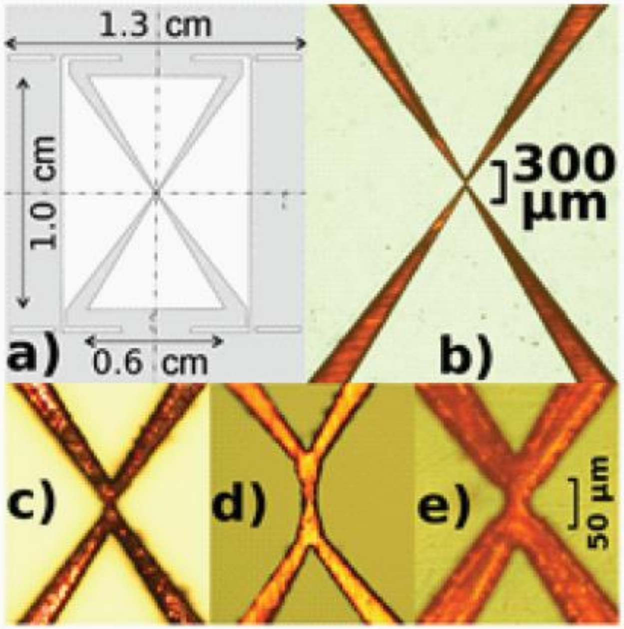

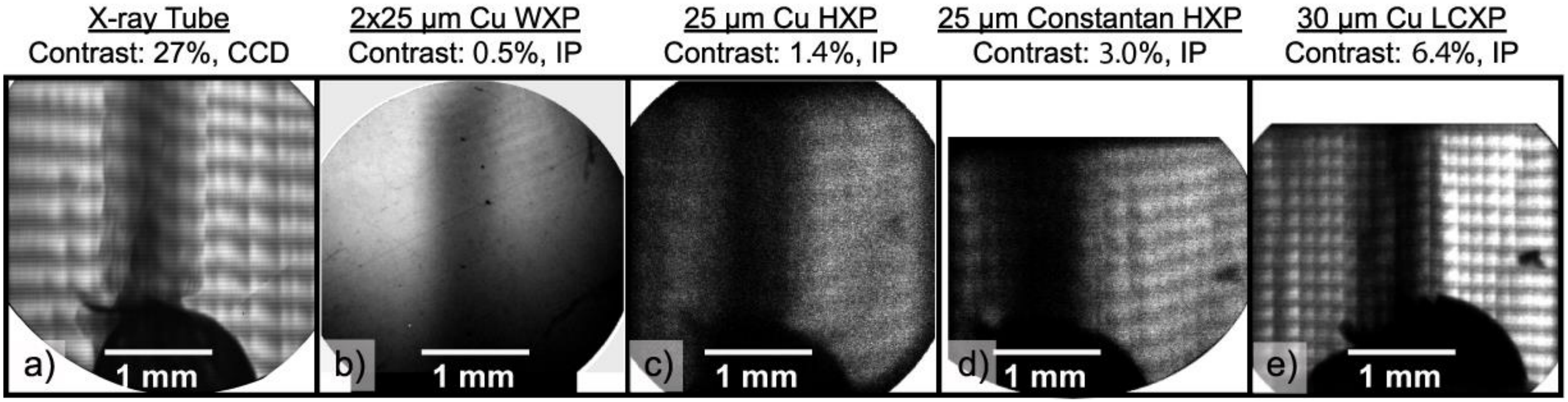

X-pinch x-ray sources for TXD: M. P. Valdivia, *PPCF* **64** (2022)

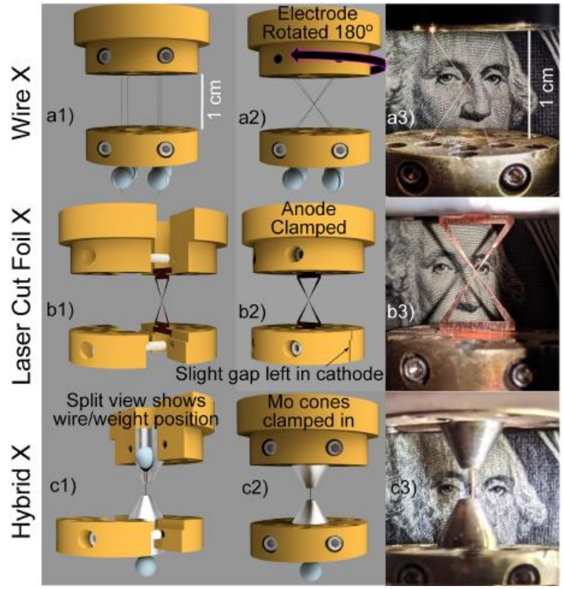

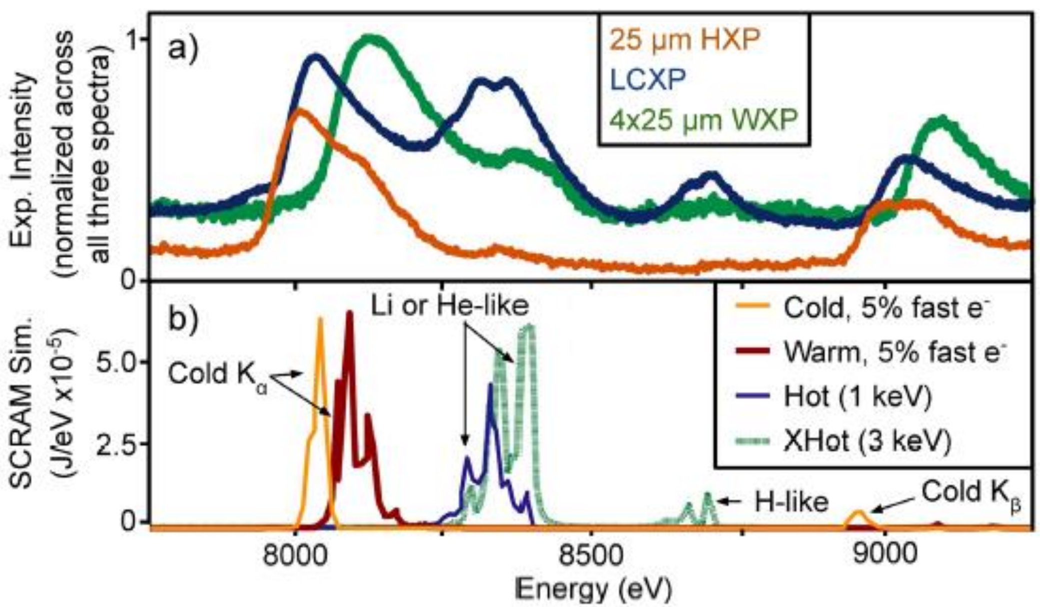

X-pinch emission: G. Collins, et al., *J. Appl. Phys.* **129** (2021)

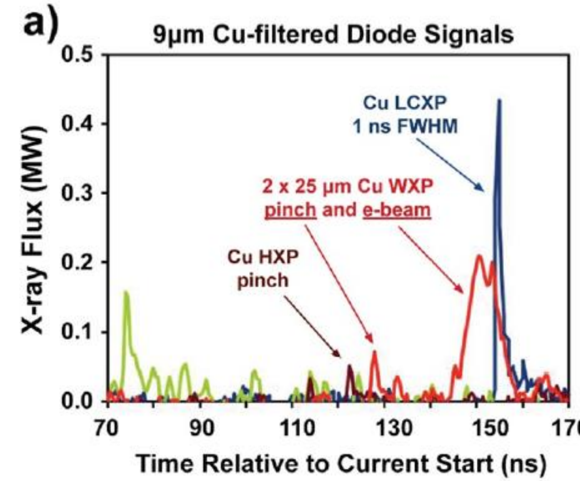

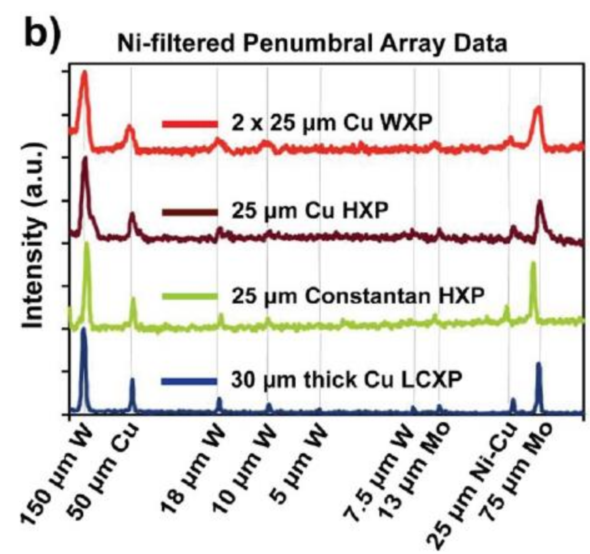

X-pinch for TXD: M. P. Valdivia, *PPCF* **64** (2022)

- Laser-cut x-pinches deliver reproducible single point-source 8 keV emission <10 μm. Laser-cut emission used to image 2 x 25 μm Al wire x-pinch driven by the return current.

- Wire core expansion was imaged for the first time using Talbot-Lau interferometry in the Moire deflectometry mode. Refraction angles (n_e gradient) high, thus fringes are hard to track. Al too transparent while W too attenuating, hence, Cu is a better sample.

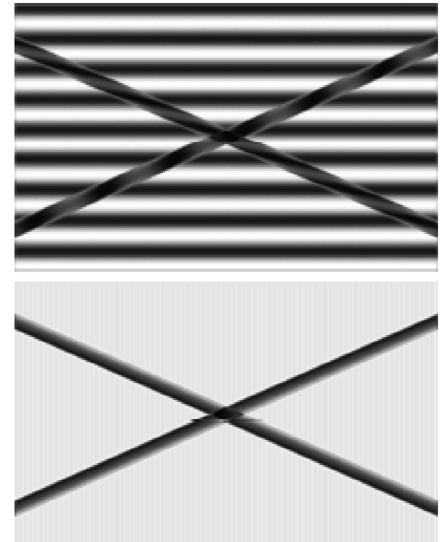

Figure 23: Simulations of 100 μm Al XP.
a) Moire. b) Refraction Enhancement.

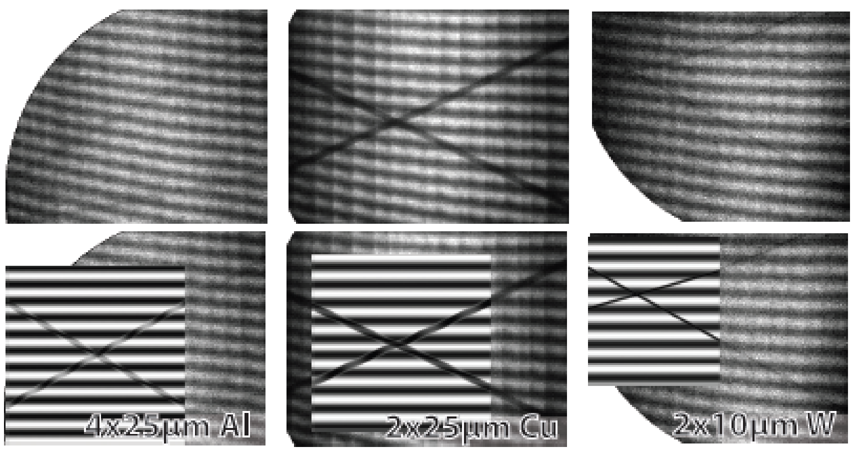

Figure 24: Al, Cu, and W x-pinch imaged by 25 μm Cu laser-cut XP (top). XWFP simulation overlapped (bottom).

- Results provide good scaling to asses TLX performance for larger pulsed-power generators. Potential as MagLIF diagnostic: Liners are opaque to visible light but transparent to x-rays: TLX can provide high resolution n_e mapping through deflectometry or Refraction Enhancement.

X-pinch x-ray sources for TXD: M. P. Valdivia, *PPCF* **64** (2022)